

ACT-06-09, MIFP-09-23

Flipped $SU(5) \times U(1)_X$ Models from F-Theory

Jing Jiang,¹ Tianjun Li,^{2,3} Dimitri V. Nanopoulos,^{2,4,5} and Dan Xie²¹*Department of Physics, University of Wisconsin, Madison, WI 53706, USA*²*George P. and Cynthia W. Mitchell Institute for Fundamental Physics,
Texas A&M University, College Station, TX 77843, USA*³*Key Laboratory of Frontiers in Theoretical Physics, Institute of Theoretical Physics,
Chinese Academy of Sciences, Beijing 100190, P. R. China*⁴*Astroparticle Physics Group, Houston Advanced Research Center (HARC),
Mitchell Campus, Woodlands, TX 77381, USA*⁵*Academy of Athens, Division of Natural Sciences,
28 Panepistimiou Avenue, Athens 10679, Greece*

(Dated: May 25, 2018)

Abstract

We systematically construct flipped $SU(5) \times U(1)_X$ models without and with bulk vector-like particles from F-theory. To realize the decoupling scenario, we introduce sets of vector-like particles in complete $SU(5) \times U(1)$ multiplets at the TeV scale, or at the intermediate scale, or at the TeV scale and high scale. To avoid the Landau pole problem for the gauge couplings, we can only introduce five sets of vector-like particles around the TeV scale. These vector-like particles can couple to the Standard Model singlet fields, and obtain suitable masses by Higgs mechanism. We study gauge coupling unification in detail. We show that the $U(1)_X$ flux contributions to the gauge couplings preserve the $SU(5) \times U(1)_X$ gauge coupling unification. We calculate the $SU(3)_C \times SU(2)_L$ unification scales, and the $SU(5) \times U(1)_X$ unification scales and unified couplings. In most of our models, the high-scale or bulk vector-like particles can be considered as string-scale threshold corrections since their masses are close to the string scale. Furthermore, we discuss the phenomenological consequences of our models. In particular, in the models with TeV-scale vector-like particles, the vector-like particles can be observed at the Large Hadron collider, the proton decay is within the reach of the future Hyper-Kamiokande experiment, the lightest CP-even Higgs boson mass can be increased, the hybrid inflation can be naturally realized, and the correct cosmic primordial density fluctuations can be generated.

PACS numbers: 11.10.Kk, 11.25.Mj, 11.25.-w, 12.60.Jv

arXiv:0905.3394v2 [hep-th] 6 Jan 2010

I. INTRODUCTION

The goal of string phenomenology is to construct realistic string models with moduli stabilization and without chiral exotics, and then make clean predictions that can be tested at the Large Hadron Collider (LHC) and other future experiments. As we know, there are three kinds of string models which have been studied extensively

(1) Heterotic $E_8 \times E_8$ string model building. The supersymmetric Standard Model (SM) can be constructed via the orbifold compactifications [1–3] and the Calabi-Yau manifold compactifications [4, 5]. The orbifold compactifications are based on the weakly coupled heterotic $E_8 \times E_8$ string theory, and the Minimal Supersymmetric Standard Model (MSSM) without chiral exotic particles can be constructed [1, 2]. However, the gauge coupling unification scale in the MSSM is around 2×10^{16} GeV [6], while the string scale M_{string} in the weakly coupled heterotic string theory is [7]

$$M_{\text{string}} = g_{\text{string}} \times 5.27 \times 10^{17} \text{ GeV} , \quad (1)$$

where g_{string} is the string coupling constant. Note that $g_{\text{string}} \sim \mathcal{O}(1)$, we have

$$M_{\text{string}} \approx 5 \times 10^{17} \text{ GeV} . \quad (2)$$

Thus, there exists a factor of approximately 20 to 25 between the MSSM unification scale and the string scale. This problem can be solved in the strong coupled heterotic $E_8 \times E_8$ string theory or M-theory on S^1/Z_2 [8] with Calabi-Yau manifold compactifications since the eleventh dimension can be relatively large about 10^{14} GeV [9], and the Grand Unified Theories (GUTs) can be realized [4, 5]. To break the GUT group via the Wilson line mechanism, the fundamental group of the Calabi-Yau manifolds should be non-trivial. Although the desirable Calabi-Yau manifolds can be constructed [4, 5], there do exist the following problems: the vanishing down-type quark Yukawa couplings; the possible R-parity violations; and the extra massless $U(1)$ if the rank of GUT group is five or higher.

(2) Free fermionic string model building. Realistic models with clean particle spectra can only be constructed at the Kac-Moody level one [10–14]. Note that the Higgs fields in the adjoint representation or higher can not be generated at the Kac-Moody level one, only three kinds of models can be constructed: the Standard-like models, Pati-Salam models, and flipped $SU(5)$ models [10–14].

(3) D-brane model building. There are two kinds of such models: (i) Intersecting D-brane models [15–23]; (ii) Orientifolds of Gepner models [24, 25]. The standard-like models, Pati-Salam models, trinification models, $SU(5)$ models, as well as flipped $SU(5)$ models have been constructed [16–22, 24, 25]. However, in the trinification models, $SU(5)$ models, and flipped $SU(5)$ models, some of the SM fermion Yukawa couplings are forbidden due to

the remaining global $U(1)$ symmetries at the perturbative level, for example, the up-type quark Yukawa couplings $\mathbf{10}_i\mathbf{10}_j\mathbf{5}_H$ in the $SU(5)$ model. This problem might be solved in the Type IIB orientifold compactifications [26] due to non-perturbative instanton effects [27]. In the standard-like models and Pati-Salam models, we can have all the SM fermion Yukawa couplings at the stringy tree level in principle. However, there are some problems in the generic standard-like models and Pati-Salam models: rank-one problem in the SM fermion Yukawa coupling matrices, no gauge coupling unification, and additional exotic particles, etc. These problems can be solved only in a few models [28, 29].

On the other hand, there are strong indications favoring GUTs from the known low-energy particle physics. The gauge couplings in the MSSM are indeed unified at the GUT scale M_{GUT} around 2×10^{16} GeV [6]. Moreover, one family of the SM fermions forms the $\mathbf{10}$ and $\bar{\mathbf{5}}$ representations in $SU(5)$ models and a single spinor $\mathbf{16}$ representation in $SO(10)$ models. Especially, we indeed can have the Yukawa coupling unification for the third family of the SM fermions [30]. Also, GUTs can explain charge quantization naturally, etc. Therefore, it is very interesting to construct GUTs especially $SO(10)$ models from the string theory.

Recently, semi-realistic GUTs have been constructed locally in the F-theory with seven-branes, which can be considered as the strongly coupled formulation of ten-dimensional Type IIB string theory with a varying axion (a)-dilaton (ϕ) field $\tau = a + ie^{-\phi}$ [31–35] (For a briefly review, see Section III.). Then further model building and phenomenological consequences have been studied extensively [36–57]. Note that the known GUTs without additional chiral exotic particles are asymptotically free, and asymptotic freedom can be translated into the existence of a consistent decompactification limit. Also, the Planck scale M_{Pl} is about 10^{19} GeV, so, $M_{\text{GUT}}/M_{\text{Pl}}$ is indeed a small number around $10^{-3} - 10^{-2}$. Thus, it is natural to assume that $M_{\text{GUT}}/M_{\text{Pl}}$ is small from the effective field theory point of view in the bottom-up approach, and then gravity can be decoupled. In the decoupling limit where $M_{\text{Pl}} \rightarrow \infty$ while M_{GUT} remains finite, semi-realistic $SU(5)$ models and $SO(10)$ models without chiral exotic particles have been constructed locally. To decouple gravity and avoid the bulk matter fields on the observable seven-branes, we can show that the observable seven-branes should wrap a del Pezzo n surface dP_n with $n \geq 2$ for the internal space dimensions (For a review of del Pezzo n surfaces, see Appendix A.) [33, 34]. The GUT gauge fields are on the worldvolume of the observable seven-branes, while the matter and Higgs fields are localized on the codimension-one curves in dP_n . A brand new feature is that the $SU(5)$ and $SO(10)$ gauge symmetries can be broken down to the SM and $SU(5) \times U(1)$ gauge symmetries, respectively by turning on $U(1)$ fluxes. Because the $SO(10)$ models have not only gauge interaction unification but also fermion unification, it seems to us that $SO(10)$ models is more interesting than $SU(5)$. In the $SO(10)$ models, to eliminate the zero modes of the chiral exotic particles, we must break the $SO(10)$ gauge symmetry down to the flipped

$SU(5) \times U(1)_X$ gauge symmetry [34]. Interestingly, in flipped $SU(5) \times U(1)_X$ models [58, 59], we can solve the doublet-triplet splitting problem via the missing partner mechanism [60].

In flipped $SU(5) \times U(1)_X$ models of $SO(10)$ origin, there are two unification scales: the $SU(2)_L \times SU(3)_C$ unification scale M_{23} and the $SU(5) \times U(1)_X$ unification scale M_U where M_{23} is about the usual GUT scale around 2×10^{16} GeV. To solve the little hierarchy problem between the GUT scale and string scale M_{string} , we have introduced extra vector-like particles, and achieved the string-scale gauge coupling unification in flipped $SU(5) \times U(1)_X$ models [61, 62]. Similarly, for the flipped $SU(5) \times U(1)_X$ models from F-theory, we can naturally obtain the decoupling scenario where M_{23}/M_U or M_{23}/M_{Pl} can be small by introducing the additional vector-like particles.

In this paper, we briefly review the flipped $SU(5) \times U(1)_X$ models with string-scale gauge coupling unification [61, 62]. We also review the F-theory model building. To separate the mass scales M_{23} and M_U and realize the decoupling scenario, we introduce sets of vector-like particles in complete $SU(5) \times U(1)_X$ multiplets, whose contributions to the one-loop beta functions of the $U(1)_Y$, $SU(2)_L$ and $SU(3)_C$ gauge symmetries, Δb_1 , Δb_2 and Δb_3 respectively, satisfy $\Delta b_1 < \Delta b_2 = \Delta b_3$. To avoid the Landau pole problem for the gauge couplings, we can only introduce five sets of vector-like particles around the TeV scale which could be observed at the LHC. Moreover, we systematically construct the flipped $SU(5) \times U(1)_X$ models without bulk vector-like particles: (i) Type I models only have the vector-like particles around the TeV scale; (ii) Type II models only have the vector-like particles at the intermediate scale; (iii) Type III models have the vector-like particles around the TeV scale and the high scale (for definitions, see Section IV). For a complete study, we also construct the Type I, Type II and Type III models with one pair and two pairs of bulk vector-like particles on the observable seven-branes. Interestingly, these vector-like particles can couple to the SM singlet fields, and can obtain masses about from the TeV scale to the GUT scale via Higgs mechanism. In addition, we study the gauge coupling unification in all of our models without bulk vector-like particles, and in the Type IA and Type IIA models (for definitions, see Sections IV and V) with bulk vector-like particles. We also study string-scale gauge coupling unification defined in Eq. 1 in the Type III models, and the Type IA and Type IIA models with bulk vector-like particles. We show that the $U(1)_X$ flux contributions to the gauge couplings preserve the $SU(5) \times U(1)_X$ gauge coupling unification. We calculate the $SU(3)_C \times SU(2)_L$ unification scales, and the $SU(5) \times U(1)_X$ unification scales and unified couplings. Interestingly, in most of our models, the high-scale or bulk vector-like particles can be considered as the string-scale threshold corrections since their masses are close to the string scale. We show that the Z_0 and Z_1 sets of vector-like particles (for definitions, see Section II) can have masses below the 1 TeV scale, and then they can be produced at the LHC. Thus, the corresponding models, which have Z_0 or Z_1

sets of vector-like particles at about 1 TeV scale, can be tested at the LHC.

Furthermore, we discuss the phenomenological consequences of our models: (i) We point out that there may exist additional chiral exotic particles or vector-like particles when we embed the local F-theory GUTs into the global consistent setup. (ii) Considering suitable threshold corrections at the supersymmetry breaking scale and the M_{23} scale, we might have the Z_2 , Z_3 and Z_4 sets of vector-like particles (for definitions, see Section II) whose masses can be below the 1 TeV scale. Thus, all of our models with TeV-scale vector-like particles could be tested at the LHC. (iii) There are Yukawa interactions between the MSSM Higgs fields and the TeV-scale vector-like particles. With relatively large Yukawa couplings which are consistent with the perturbative unification, we can increase the lightest CP-even Higgs boson mass. (iv) Considering proton decay $p \rightarrow e^+\pi^0$ via dimension-6 operator from heavy gauge boson exchange and including the threshold corrections, we obtain that the proton life time in our models is smaller than 1×10^{35} years [43]. Thus, our models can definitely be tested at the future Hyper-Kamiokande proton decay experiment [63]. (v) The neutrino masses and mixings can be generated via the seesaw mechanism, and the baryon asymmetry can be explained via the leptogenesis. (vi) We can naturally realize the hybrid inflation in our models, solve the monopole problem, and obtain the correct cosmic primordial density fluctuations.

This paper is organized as follows: in Section II, we briefly review the flipped $SU(5) \times U(1)_X$ models. In Section III, we review the F-theory model buildings, and discuss the minimal flipped $SU(5) \times U(1)_X$ model. In Sections IV and V, we systematically construct the flipped $SU(5) \times U(1)_X$ models without and with bulk vector-like particles, respectively. We discuss the phenomenological consequences in Section VI. Our discussion and conclusions are in Section VI. In Appendix A, we briefly review the del Pezzo surfaces. In Appendices B and C, we present the vector-like particle curves and the gauge bundle assignments in our models with one pair and two pairs of bulk vector-like particles, respectively. In Appendix D, we give the one-loop and two-loop beta functions for the bulk vector-like particles.

II. FLIPPED $SU(5) \times U(1)_X$ MODELS

We first briefly review the minimal flipped $SU(5)$ model [58–60]. The gauge group for flipped $SU(5)$ model is $SU(5) \times U(1)_X$, which can be embedded into $SO(10)$ model. We define the generator $U(1)_{Y'}$ in $SU(5)$ as

$$T_{U(1)_{Y'}} = \text{diag} \left(-\frac{1}{3}, -\frac{1}{3}, -\frac{1}{3}, \frac{1}{2}, \frac{1}{2} \right). \quad (3)$$

The hypercharge is given by

$$Q_Y = \frac{1}{5} (Q_X - Q_{Y'}) . \quad (4)$$

There are three families of the SM fermions whose quantum numbers under $SU(5) \times U(1)_X$ are

$$F_i = (\mathbf{10}, \mathbf{1}), \quad \bar{f}_i = (\bar{\mathbf{5}}, -\mathbf{3}), \quad \bar{l}_i = (\mathbf{1}, \mathbf{5}), \quad (5)$$

where $i = 1, 2, 3$. The SM particle assignments in F_i , \bar{f}_i and \bar{l}_i are

$$F_i = (Q_i, D_i^c, N_i^c), \quad \bar{f}_i = (U_i^c, L_i), \quad \bar{l}_i = E_i^c , \quad (6)$$

where Q_i and L_i are respectively the superfields of the left-handed quark and lepton doublets, U_i^c , D_i^c , E_i^c and N_i^c are the CP conjugated superfields for the right-handed up-type quarks, down-type quarks, leptons and neutrinos, respectively. To generate the heavy right-handed neutrino masses, we introduce three SM singlets ϕ_i .

To break the GUT and electroweak gauge symmetries, we introduce two pairs of Higgs representations

$$H = (\mathbf{10}, \mathbf{1}), \quad \bar{H} = (\bar{\mathbf{10}}, -\mathbf{1}), \quad h = (\mathbf{5}, -\mathbf{2}), \quad \bar{h} = (\bar{\mathbf{5}}, \mathbf{2}). \quad (7)$$

We label the states in the H multiplet by the same symbols as in the F multiplet, and for \bar{H} we just add “bar” above the fields. Explicitly, the Higgs particles are

$$H = (Q_H, D_H^c, N_H^c) , \quad \bar{H} = (\bar{Q}_{\bar{H}}, \bar{D}_{\bar{H}}^c, \bar{N}_{\bar{H}}^c) , \quad (8)$$

$$h = (D_h, D_h, D_h, H_d) , \quad \bar{h} = (\bar{D}_{\bar{h}}, \bar{D}_{\bar{h}}, \bar{D}_{\bar{h}}, H_u) , \quad (9)$$

where H_d and H_u are one pair of Higgs doublets in the MSSM. We also add one singlet Φ .

To break the $SU(5) \times U(1)_X$ gauge symmetry down to the SM gauge symmetry, we introduce the following Higgs superpotential at the GUT scale

$$W_{\text{GUT}} = \lambda_1 H H h + \lambda_2 \bar{H} \bar{H} \bar{h} + \Phi (\bar{H} H - M_{\text{H}}^2) . \quad (10)$$

There is only one F-flat and D-flat direction, which can always be rotated along the N_H^c and $\bar{N}_{\bar{H}}^c$ directions. So, we obtain that $\langle N_H^c \rangle = \langle \bar{N}_{\bar{H}}^c \rangle = M_{\text{H}}$. In addition, the superfields H and \bar{H} are eaten and acquire large masses via the supersymmetric Higgs mechanism, except for D_H^c and $\bar{D}_{\bar{H}}^c$. And the superpotential $\lambda_1 H H h$ and $\lambda_2 \bar{H} \bar{H} \bar{h}$ couple the D_H^c and $\bar{D}_{\bar{H}}^c$ with the D_h and $\bar{D}_{\bar{h}}$, respectively, to form the massive eigenstates with masses $2\lambda_1 \langle N_H^c \rangle$ and $2\lambda_2 \langle \bar{N}_{\bar{H}}^c \rangle$. So, we naturally have the doublet-triplet splitting due to the missing partner

mechanism [60]. Because the triplets in h and \bar{h} only have small mixing through the μ term, the Higgsino-exchange mediated proton decay are negligible, *i.e.*, we do not have the dimension-5 proton decay problem.

The SM fermion masses are from the following superpotential

$$W_{\text{Yukawa}} = y_{ij}^D F_i F_j h + y_{ij}^{U\nu} F_i \bar{f}_j \bar{h} + y_{ij}^E \bar{l}_i \bar{f}_j h + \mu h \bar{h} + y_{ij}^N \phi_i \bar{H} F_j , \quad (11)$$

where y_{ij}^D , $y_{ij}^{U\nu}$, y_{ij}^E and y_{ij}^N are Yukawa couplings, and μ is the bilinear Higgs mass term.

After the $SU(5) \times U(1)_X$ gauge symmetry is broken down to the SM gauge symmetry, the above superpotential gives

$$W_{SSM} = y_{ij}^D D_i^c Q_j H_d + y_{ji}^{U\nu} U_i^c Q_j H_u + y_{ij}^E E_i^c L_j H_d + y_{ij}^{U\nu} N_i^c L_j H_u \\ + \mu H_d H_u + y_{ij}^N \langle \bar{N}_i^c / \bar{H} \rangle \phi_i N_j^c + \dots \text{(decoupled below } M_{GUT}\text{)}. \quad (12)$$

Similar to the flipped $SU(5) \times U(1)_X$ models with string-scale gauge coupling unification [61, 62], we introduce vector-like particles which form the complete flipped $SU(5) \times U(1)_X$ multiplets. The quantum numbers for these additional vector-like particles under the $SU(5) \times U(1)_X$ gauge symmetry are

$$XF = (\mathbf{10}, \mathbf{1}) , \quad \overline{XF} = (\overline{\mathbf{10}}, -\mathbf{1}) , \quad (13)$$

$$Xf = (\mathbf{5}, \mathbf{3}) , \quad \overline{Xf} = (\overline{\mathbf{5}}, -\mathbf{3}) , \quad (14)$$

$$Xl = (\mathbf{1}, -\mathbf{5}) , \quad \overline{Xl} = (\mathbf{1}, \mathbf{5}) , \quad (15)$$

$$Xh = (\mathbf{5}, -\mathbf{2}) , \quad \overline{Xh} = (\overline{\mathbf{5}}, \mathbf{2}) , \quad (16)$$

$$XT = (\mathbf{10}, -\mathbf{4}) , \quad \overline{XT} = (\overline{\mathbf{10}}, \mathbf{4}) . \quad (17)$$

Moreover, the particle contents from the decompositions of XF , \overline{XF} , Xf , \overline{Xf} , Xl , \overline{Xl} , Xh , \overline{Xh} , XF , and \overline{XT} , under the SM gauge symmetry are

$$XF = (XQ, XD^c, XN^c) , \quad \overline{XF} = (XQ^c, XD, XN) , \quad (18)$$

$$Xf = (XU, XL^c) , \quad \overline{Xf} = (XU^c, XL) , \quad (19)$$

$$Xl = XE , \quad \overline{Xl} = XE^c , \quad (20)$$

$$Xh = (XD, XL) , \quad \overline{Xh} = (XD^c, XL^c) , \quad (21)$$

$$XT = (XY, XU^c, XE) , \quad \overline{XT} = (XY^c, XU, XE^c) . \quad (22)$$

Under the $SU(3)_C \times SU(2)_L \times U(1)_Y$ gauge symmetry, the quantum numbers for the extra

vector-like particles are

$$XQ = (\mathbf{3}, \mathbf{2}, \frac{1}{6}), \quad XQ^c = (\bar{\mathbf{3}}, \mathbf{2}, -\frac{1}{6}), \quad (23)$$

$$XU = (\mathbf{3}, \mathbf{1}, \frac{2}{3}), \quad XU^c = (\bar{\mathbf{3}}, \mathbf{1}, -\frac{2}{3}), \quad (24)$$

$$XD = (\mathbf{3}, \mathbf{1}, -\frac{1}{3}), \quad XD^c = (\bar{\mathbf{3}}, \mathbf{1}, \frac{1}{3}), \quad (25)$$

$$XL = (\mathbf{1}, \mathbf{2}, -\frac{1}{2}), \quad XL^c = (\mathbf{1}, \mathbf{2}, \frac{1}{2}), \quad (26)$$

$$XE = (\mathbf{1}, \mathbf{1}, -1), \quad XE^c = (\mathbf{1}, \mathbf{1}, 1), \quad (27)$$

$$XN = (\mathbf{1}, \mathbf{1}, \mathbf{0}), \quad XN^c = (\mathbf{1}, \mathbf{1}, \mathbf{0}), \quad (28)$$

$$XY = (\mathbf{3}, \mathbf{2}, -\frac{5}{6}), \quad XY^c = (\bar{\mathbf{3}}, \mathbf{2}, \frac{5}{6}). \quad (29)$$

To separate the mass scales M_{23} and M_U in our F-theory flipped $SU(5) \times U(1)_X$ models, we need to introduce sets of vector-like particles around the TeV scale or intermediate scale whose contributions to the one-loop beta functions satisfy $\Delta b_1 < \Delta b_2 = \Delta b_3$. To avoid the Landau pole problem, we have shown that there are only five possible such sets of vector-like particles as follows due to the quantizations of the one-loop beta functions [62]

$$Z0 : XF + \overline{XF}; \quad (30)$$

$$Z1 : XF + \overline{XF} + Xl + \overline{Xl}; \quad (31)$$

$$Z2 : XF + \overline{XF} + Xf + \overline{Xf}; \quad (32)$$

$$Z3 : XF + \overline{XF} + Xl + \overline{Xl} + Xh + \overline{Xh}; \quad (33)$$

$$Z4 : XF + \overline{XF} + Xh + \overline{Xh}. \quad (34)$$

Thus, we will construct the flipped $SU(5) \times U(1)_X$ models with these sets of vector-like particles around the TeV scale, and two models respectively with $Z0$ and $Z4$ sets at the intermediate scale.

III. F-THEORY MODEL BUILDING

We first briefly review the F-theory model building [31–35]. The twelve-dimensional F theory is a convenient way to describe Type IIB vacua with varying axion-dilaton $\tau = a + ie^{-\phi}$. We compactify F-theory on a Calabi-Yau fourfold, which is elliptically fibered $\pi : Y_4 \rightarrow B_3$ with a section $\sigma : B_3 \rightarrow Y_4$. The base B_3 is the internal space dimensions in Type IIB string theory, and the complex structure of the T^2 fibre encodes τ at each point of B_3 . The SM or GUT gauge theories are on the worldvolume of the observable seven-branes that wrap a complex codimension-one surface in B_3 . Denoting the complex

coordinate tranverse to these seven-branes in B_3 as z , we can write the elliptic fibration in Weierstrass form

$$y^2 = x^3 + f(z)x + g(z) , \quad (35)$$

where $f(z)$ and $g(z)$ are sections of $K_{B_3}^{-4}$ and $K_{B_3}^{-6}$, respectively. The complex structure of the fibre is

$$j(\tau) = \frac{4(24f)^3}{\Delta} , \quad \Delta = 4f^3 + 27g^2 . \quad (36)$$

At the discriminant locus $\{\Delta = 0\} \subset B_3$, the torus T^2 degenerates by pinching one of its cycles and becomes singular. For a generic pinching one-cycle $(p, q) = p\alpha + q\beta$ where α and β are one-cycles for the torus T^2 , we obtain a (p, q) seven-brane in the locus where the (p, q) string can end. The singularity types of the elliptically fibres fall into the familiar *ADE* classifications, and we identify the corresponding *ADE* gauge groups on the seven-brane world-volume. This is one of the most important advantages for the F-theory model building: the exceptional gauge groups appear rather naturally, which is absent in perturbative Type II string theory. And then all the SM fermion Yukawa couplings in the GUTs can be generated.

We assume that the observable seven-branes with GUT models on its worldvolume wrap a complex codimension-one surface S in B_3 , and the observable gauge symmetry is G_S . When $h^{1,0}(S) \neq 0$, the low energy spectrum may contain the extra states obtained by reduction of the bulk supergravity modes of compactification. So we require that $\pi_1(S)$ be a finite group. In order to decouple gravity and construct models locally, the extension of the local metric on S to a local Calabi-Yau fourfold must have a limit where the surface S can be shrunk to zero size. This implies that the anti-canonical bundle on S must be ample. Therefore, S is a del Pezzo n surface dP_n with $n \geq 2$ in which $h^{2,0}(S) = 0$. By the way, the Hirzebruch surfaces with degree larger than 2 satisfy $h^{2,0}(S) = 0$ but do not define the fully consistent decoupled models [33, 34].

To describe the spectrum, we have to study the gauge theory of the worldvolume on the seven-branes. We start from the maximal supersymmetric gauge theory on $\mathbb{R}^{3,1} \times \mathbb{C}^2$ and then replace \mathbb{C}^2 with the Kähler surface S . In order to have four-dimensional $\mathcal{N} = 1$ supersymmetry, the maximal supersymmetric gauge theory on $\mathbb{R}^{3,1} \times \mathbb{C}^2$ should be twisted. It was shown that there exists a unique twist preserving $\mathcal{N} = 1$ supersymmetry in four dimensions, and chiral matters can arise from the bulk S or the codimension-one curve Σ in S which is the intersection between the observable seven-branes and the other seven-brane(s) [33, 34].

In order to have the matter fields on S , we consider a non-trivial vector bundle on S with a structure group H_S which is a subgroup of G_S . Then the gauge group G_S is broken down

to $\Gamma_S \times H_S$, and the adjoint representation $\text{ad}(G_S)$ of the G_S is decomposed as

$$\text{ad}(G_S) \rightarrow \text{ad}(\Gamma_S) \bigoplus \text{ad}(H_S) \bigoplus_j (\tau_j, T_j) . \quad (37)$$

Employing the vanishing theorem of the del Pezzo surfaces, we obtain the numbers of the generations and anti-generations by calculating the zero modes of the Dirac operator on S

$$n_{\tau_j} = -\chi(S, \mathbf{T}_j) , \quad n_{\tau_j^*} = -\chi(S, \mathbf{T}_j^*) , \quad (38)$$

where \mathbf{T}_j is the vector bundle on S whose sections transform in the representation T_j of H_S , and \mathbf{T}_j^* is the dual bundle of \mathbf{T}_j . In particular, when the H_S bundle is a line bundle L , we have

$$n_{\tau_j} = -\chi(S, L^j) = -\left[1 + \frac{1}{2}\left(\int_S c_1(L^j)c_1(S) + \int_S c_1(L^j)^2\right)\right] . \quad (39)$$

In order to preserve supersymmetry, the line bundle L should satisfy the BPS equation [33]

$$J_S \wedge c_1(L) = 0, \quad (40)$$

where J_S is the Kähler form on S . Moreover, the admissible supersymmetric line bundles on del Pezzo surfaces must satisfy $c_1(L)c_1(S) = 0$, thus, $n_{\tau_j} = n_{\tau_j^*}$ and only the vector-like particles can be obtained. In short, we can not have the chiral matter fields on the worldvolume of the observable seven-branes.

Interestingly, the chiral superfields can come from the intersections between the observable seven-branes and the other seven-brane(s) [33, 34]. Let us consider a stack of seven-branes with gauge group $G_{S'}$ that wrap a codimension-one surface S' in B_3 . The intersection of S and S' is a codimension-one curve (Riemann surface) Σ in S and S' , and the gauge symmetry on Σ will be enhanced to G_Σ where $G_\Sigma \supset G_S \times G_{S'}$. On this curve, there exist chiral matters from the decomposition of the adjoint representation $\text{ad}G_\Sigma$ of G_Σ as follows

$$\text{ad}G_\Sigma = \text{ad}G_S \oplus \text{ad}G_{S'} \oplus_k (U_k \otimes U'_k) . \quad (41)$$

Turning on the non-trivial gauge bundles on S and S' respectively with structure groups H_S and $H_{S'}$, we break the gauge group $G_S \times G_{S'}$ down to the commutant subgroup $\Gamma_S \times \Gamma_{S'}$. Defining $\Gamma \equiv \Gamma_S \times \Gamma_{S'}$ and $H \equiv H_S \times H_{S'}$, we can decompose $U \otimes U'$ into the irreducible representations as follows

$$U \otimes U' = \bigoplus_k (r_k, V_k), \quad (42)$$

where r_k and V_k are the representations of Γ and H , respectively. The light chiral fermions in the representation r_k are determined by the zero modes of the Dirac operator on Σ . The net number of chiral superfields is given by

$$N_{r_k} - N_{r_k^*} = \chi(\Sigma, K_\Sigma^{1/2} \otimes \mathbf{V}_k), \quad (43)$$

where K_Σ is the restriction of canonical bundle on the curve Σ , and \mathbf{V}_k is the vector bundle whose sections transform in the representation V_k of the structure group H .

In the F-theory model building, we are interested in the models where $G_{S'}$ is $U(1)'$, and H_S and $H_{S'}$ are respectively $U(1)$ and $U(1)'$. Then the vector bundles on S and S' are line bundles L and L' . The adjoint representation $\text{ad}G_\Sigma$ of G_Σ is decomposed into a direct sum of the irreducible representations under the group $\Gamma_S \times U(1) \times U(1)'$ that can be denoted as $(\mathbf{r}_j, \mathbf{q}_j, \mathbf{q}'_j)$

$$\text{ad}G_\Sigma = \text{ad}(\Gamma_S) \oplus \text{ad}G_{S'} \oplus_j (\mathbf{r}_j, \mathbf{q}_j, \mathbf{q}'_j) . \quad (44)$$

The numbers of chiral supefields in the representation $(\mathbf{r}_j, \mathbf{q}_j, \mathbf{q}'_j)$ and their Hermitian conjugates on the curve Σ are given by

$$N_{(\mathbf{r}_j, \mathbf{q}_j, \mathbf{q}'_j)} = h^0(\Sigma, \mathbf{V}_j) , \quad N_{(\bar{\mathbf{r}}_j, -\mathbf{q}_j, -\mathbf{q}'_j)} = h^1(\Sigma, \mathbf{V}_j) , \quad (45)$$

where

$$\mathbf{V}_j = K_\Sigma^{1/2} \otimes L_\Sigma^{\mathbf{q}_j} \otimes L'^{\mathbf{q}'_j} , \quad (46)$$

where $K_\Sigma^{1/2}$, $L_\Sigma^{\mathbf{r}_j}$ and $L'^{\mathbf{q}'_j}$ are the restrictions of canonical bundle K_S , line bundles L and L' on the curve Σ , respectively. In particular, if the volume of S' is infinite, $G_{S'} = U(1)'$ is decoupled. And then the index \mathbf{q}'_j can be ignored.

Using Riemann-Roch theorem, we obtain the net number of chiral supefields in the representation $(\mathbf{r}_j, \mathbf{q}_j, \mathbf{q}'_j)$

$$N_{(\mathbf{r}_j, \mathbf{q}_j, \mathbf{q}'_j)} - N_{(\bar{\mathbf{r}}_j, -\mathbf{q}_j, -\mathbf{q}'_j)} = 1 - g + \text{deg}(\mathbf{V}_j) , \quad (47)$$

where g is the genus of the curve Σ .

Moreover, we can obtain the Yukawa couplings at the triple intersection of three curves Σ_i , Σ_j and Σ_k where the gauge group or the singularity type is enhanced further. To have the triple intersections, the corresponding homology classes $[\Sigma_i]$, $[\Sigma_j]$ and $[\Sigma_k]$ of the curves Σ_i , Σ_j and Σ_k must satisfy the following conditions

$$[\Sigma_i] \cdot [\Sigma_j] > 0 , \quad [\Sigma_i] \cdot [\Sigma_k] > 0 , \quad [\Sigma_j] \cdot [\Sigma_k] > 0 . \quad (48)$$

In this paper, we will construct flipped $SU(5) \times U(1)_X$ models systematically. Thus, we will choose $G_S = SO(10)$ and $H_S = U(1)_X$. Under $SU(5) \times U(1)_X$, the $SO(10)$ representations are decomposed as follows

$$\mathbf{10} = (\mathbf{5}, -2) \oplus (\bar{\mathbf{5}}, 2) , \quad (49)$$

$$\mathbf{16} = (\mathbf{10}, 1) \oplus (\bar{\mathbf{5}}, -3) \oplus (\mathbf{1}, 5) , \quad (50)$$

$$\mathbf{45} = (\mathbf{24}, 0) \oplus (\mathbf{1}, 0) \oplus (\mathbf{10}, -4) \oplus (\bar{\mathbf{10}}, 4) . \quad (51)$$

Moreover, the Higgs fields h and \bar{h} and the vector-like particles Xh and $\overline{X\bar{h}}$ are on the curves where the $SO(10)$ gauge symmetry is enhanced to $SO(12)$. Under $SO(10) \times U(1)$, the adjoint representation of $SO(12)$ is decomposed as follows

$$\mathbf{66} = (\mathbf{45}, \mathbf{0}) \oplus (\mathbf{1}, \mathbf{0}) \oplus (\mathbf{10}, \mathbf{2}) \oplus (\overline{\mathbf{10}}, -\mathbf{2}) . \quad (52)$$

All the other fields in our models are on the curves where the $SO(10)$ gauge symmetry is enhanced to E_6 . Under $SO(10) \times U(1)$, the adjoint representation of E_6 is decomposed as follows

$$\mathbf{78} = (\mathbf{45}, \mathbf{0}) \oplus (\mathbf{1}, \mathbf{0}) \oplus (\mathbf{16}, \mathbf{3}) \oplus (\overline{\mathbf{16}}, -\mathbf{3}) . \quad (53)$$

In addition, the SM fermion Yukawa couplings in our models arise from the triple intersections where the gauge symmetry is enhanced to E_7 .

In this paper, we consider the del Pezzo 8 surface dP_8 . In the Section IV, we will choose the line bundle $L = \mathcal{O}_S(E_1 - E_2)^{1/4}$, and construct the flipped $SU(5) \times U(1)_X$ models without bulk vector-like particles XT_i and $\overline{X\bar{T}_i}$. Moreover, in the Section V, we will choose the line bundles as $L = \mathcal{O}_S(E_1 - E_2 + E_4 - E_5)^{1/4}$ and $L = \mathcal{O}_S(E_1 - E_2 + E_4 - E_5 + E_6 - E_7)^{1/4}$, and we construct the flipped $SU(5) \times U(1)_X$ models with one and two pairs of bulk vector-like particles XT_i and $\overline{X\bar{T}_i}$, respectively.

In our model building, the SM fermion and Higgs curves with homology classes and the gauge bundle assignments for each curve in the minimal flipped $SU(5) \times U(1)_X$ model are universal in all of our models and are given in Table I. In short, all three generations localize on the matter curve Σ_F which is pinched. Because the homology classes for the SM fermion and Higgs curves satisfy Eq. (48), the SM fermion Yukawa couplings are allowed. There are singlets in the models from the intersections of the other seven-branes as well. For simplicity, in the following discussions, we will assume the universal supersymmetry breaking, and denote the supersymmetry breaking scale as M_S .

Particles	Curve	Class	g_Σ	L_Σ	L_Σ^n
h	Σ_h	$2H - E_2 - E_3$	0	$\mathcal{O}_{\Sigma_H^{(d)}}(-1)^{1/4}$	$\mathcal{O}_{\Sigma_H^{(d)}}(1)^{1/2}$
\bar{h}	$\Sigma_{\bar{h}}$	$2H - E_1 - E_3$	0	$\mathcal{O}_{\Sigma_H^{(u)}}(1)^{1/4}$	$\mathcal{O}_{\Sigma_H^{(u)}}(-1)^{1/2}$
16_i	Σ_F (pinched)	$3H$	1	\mathcal{O}_{Σ_F}	$\mathcal{O}_{\Sigma_F}(3p')$
$(H + \overline{H})$	Σ_H (pinched)	$3H - E_1 - E_2$	1	$\mathcal{O}_{\Sigma_H}(p_{12})^{1/4}$	$\mathcal{O}_{\Sigma_H}(p_{12})^{-1/4}$

TABLE I: The SM fermion and Higgs curves and the gauge bundle assignments for each curve in the minimal flipped $SU(5) \times U(1)_X$ model. Here $i = 1, 2, 3$, and $p_{12} = p_1 - p_2$.

In the following, we will study the gauge couplings in details. For simplicity, we will neglect the threshold corrections from the heavy KK modes [64] since their masses are around the scale M_U and higher in our F-theory flipped $SU(5) \times U(1)_X$ models. In addition, the $U(1)_X$ flux will also change the $SU(5)$ and $U(1)_X$ gauge couplings at the unification scale [35, 45]. From the particle physics point of view, only the relative changes between the gauge couplings are physically important while the total shifts for the gauge couplings are not relevant. For example, in the F-theory $SU(5)$ models with $U(1)_Y$ flux, only the $U(1)_Y$ flux contributions to the gauge couplings are relevant, and the SM gauge coupling relation at the string scale is [35, 45]

$$\alpha_1^{-1} - \alpha_3^{-1} = \frac{3}{5}(\alpha_2^{-1} - \alpha_3^{-1}) . \quad (54)$$

Let us consider the flux contributions to the gauge couplings in our F-theory flipped $SU(5) \times U(1)_X$ models. For $G = SO(10)$ gauge group, the generators T^a of $SO(10)$ are imaginary antisymmetric 10×10 matrices. In terms of the 2×2 identity matrix σ_0 and the Pauli matrices σ_i , they can be written as tensor products of 2×2 and 5×5 matrices, $(\sigma_0, \sigma_1, \sigma_3) \otimes A_5$ and $\sigma_2 \otimes S_5$ as a complete set, where A_5 and S_5 are the 5×5 real anti-symmetric and symmetric matrices [65]. In particular, the generator for $U(1)_X$ is $\sigma_2 \otimes I_5$ where I_5 is the 5×5 identity matrix. Also, the generators for flipped $SU(5) \times U(1)_X$ are [65]

$$\begin{aligned} \sigma_0 \otimes A_3, \quad \sigma_0 \otimes A_2, \quad \sigma_1 \otimes A_X \\ \sigma_2 \otimes S_3, \quad \sigma_2 \otimes S_2, \quad \sigma_3 \otimes A_X, \end{aligned} \quad (55)$$

where A_3 and S_3 are respectively the diagonal blocks of A_5 and S_5 that have indices 1, 2, and 3, while the diagonal blocks A_2 and S_2 have indices 4 and 5. A_X and S_X are the off diagonal blocks of A_5 and S_5 .

The flux contributions to the gauge couplings can be computed by dimensionally reducing the Chern-Simons action of the observable seven-branes wrapping on S

$$S_{\text{CS}} = \mu_7 \int_{S \times \mathbb{R}^{3,1}} a \wedge \text{tr}(F^4) . \quad (56)$$

In our models, the relevant flux is the $U(1)_X$ flux, which is the following

$$\langle F_{U(1)_X} \rangle = \frac{1}{2} V_{U(1)_X} \sigma_2 \otimes I_5 . \quad (57)$$

Let us normalize the $SO(10)$ generators T^a as $\text{Tr}(T^a T^b) = 2\delta_{ab}$. Then, we obtain the $U(1)_X$ flux contributions to the $SU(5)$ and $U(1)_X$ gauge couplings at the string scale in our models

$$\Delta\alpha_5^{-1} = \Delta\alpha_1'^{-1} = -\frac{1}{2}\tau \int_S c_1^2(L^4) , \quad (58)$$

where α'_1 is the $U(1)_X$ gauge coupling, and $\int_S c_1^2(L^4)$ is equal to -2 , -4 and -6 for $L = \mathcal{O}_S(E_1 - E_2)^{1/4}$, $L = \mathcal{O}_S(E_1 - E_2 + E_4 - E_5)^{1/4}$ and $L = \mathcal{O}_S(E_1 - E_2 + E_4 - E_5 + E_6 - E_7)^{1/4}$, respectively. Because there is no relevant change between the $SU(5)$ and $U(1)_X$ gauge couplings, the $U(1)_X$ flux contributions to the gauge couplings are irrelevant from the particle physics point of view. In short, including the $U(1)_X$ flux contributions to the $SU(5)$ and $U(1)_X$ gauge couplings, we still have the $SU(5) \times U(1)_X$ gauge coupling unification at the string scale.

IV. FLIPPED $SU(5) \times U(1)_X$ MODELS WITHOUT BULK VECTOR-LIKE PARTICLES

In this Section, we will take the line bundle as $L = \mathcal{O}_S(E_1 - E_2)^{1/4}$. Note that $\chi(S, L^4) = 0$, we do not have the vector-like particles XT_i and \overline{XT}_i from the bulk of the observable seven-branes. In order to separate the mass scales M_{23} and M_U in our F-theory flipped $SU(5) \times U(1)_X$ models, we introduce sets of vector-like particles around the TeV scale, or the intermediate scale, or the TeV scale and high scale. These vector-like particles can couple to the SM singlet fields from the intersections of the other seven-branes, and then obtain masses about from the TeV scale to the GUT scale by Higgs mechanism because the wave functions for the singlet fields can be attractive or repulsive and the vacuum expectation values of the singlet fields are free parameters.

A. Type I Models with TeV-Scale Vector-Like Particles

In the Type I models, the one-loop contributions to the beta functions from the sets of vector-like particles satisfy $\Delta b_2 = \Delta b_3$ and $\Delta b_2 - \Delta b_1 = 6/5$. To avoid the Landau pole problem for the gauge couplings, we can only have three models: Type IA, Type IB and Type IC models. In the Type IA model, we introduce $Z1$ set of vector-like particles. In the Type IB model, we introduce $Z2$ set of vector-like particles. And in the Type IC model, we introduce $Z3$ set of vector-like particles. Also, the curves with homology classes for the extra vector-like particles and the gauge bundle assignments for each curve in Type IA, Type IB and Type IC models are given in Table II. For simplicity, we assume that the masses for these vector-like particles are universal, and we denote the universal mass as M_V .

Using the weak-scale data in Ref. [66] and the renormalization group equations (RGEs) in Ref. [62], we study the gauge coupling unification at the two-loop level. In the Type IA models, we choose $(M_V, M_S) = (200 \text{ GeV}, 360 \text{ GeV})$, $(200 \text{ GeV}, 1000 \text{ GeV})$, $(1000 \text{ GeV}, 360 \text{ GeV})$, $(1000 \text{ GeV}, 1000 \text{ GeV})$, and $(20 \text{ TeV}, 800 \text{ GeV})$. We find that M_{23}

Model	Particles	Curve	Class	g_Σ	L_Σ	L_Σ^m
Type I & II	$(XF + \overline{XF})$	Σ_{XF} (pinched)	$3H - E_1 - E_2 - E_4$	1	$\mathcal{O}_{\Sigma_{XF}}(p_{12}^4)^{1/4}$	$\mathcal{O}_{\Sigma_{XF}}(p_{12}^4)^{-1/4}$
Type IA	$(Xl + \overline{Xl})$	Σ_{Xl} (pinched)	$3H - E_1 - E_2 - E_5$	1	$\mathcal{O}_{\Sigma_{Xl}}(p_{12}^5)^{1/4}$	$\mathcal{O}_{\Sigma_{Xl}}(p_{12}^5)^{-5/4}$
Type IB	$(Xf + \overline{Xf})$	Σ_{Xf} (pinched)	$3H - E_1 - E_2 - E_5$	1	$\mathcal{O}_{\Sigma_{Xf}}(p_{12}^5)^{1/4}$	$\mathcal{O}_{\Sigma_{Xl}}(p_{12}^5)^{3/4}$
Type IC	$(Xl + \overline{Xl})$	Σ_{Xl} (pinched)	$3H - E_1 - E_2 - E_5$	1	$\mathcal{O}_{\Sigma_{Xl}}(p_{12}^5)^{1/4}$	$\mathcal{O}_{\Sigma_{Xl}}(p_{12}^5)^{-5/4}$
	$(Xh + \overline{Xh})$	Σ_{Xh} (pinched)	$3H - E_1 - E_2 - E_6$	1	$\mathcal{O}_{\Sigma_{Xh}}(p_{12}^6)^{1/4}$	$\mathcal{O}_{\Sigma_{Xh}}(p_{12}^6)^{1/2}$
Type IIB	$(Xh + \overline{Xh})$	Σ_{Xh} (pinched)	$3H - E_1 - E_2 - E_5$	1	$\mathcal{O}_{\Sigma_{Xh}}(p_{12}^5)^{1/4}$	$\mathcal{O}_{\Sigma_{Xh}}(p_{12}^5)^{1/2}$

TABLE II: The vector-like particle curves and the gauge bundle assignments for each curve in Type I and Type II models. In particular, we have the vector-like particles (XF, \overline{XF}) in all the Type I and II models. Here, $p_{12}^m = p_1^m - p_2^m$ for $m = 4, 5, 6$, and we denote the corresponding blowing up points as p_1^m or p_2^m .

Models	M_V	M_S	M_{23}	g_U	M_U
Type IA	200	360	1.21×10^{16}	1.289	6.79×10^{17}
Type IA	200	1000	1.25×10^{16}	1.194	6.29×10^{17}
Type IA	1000	360	1.13×10^{16}	1.207	1.20×10^{18}
Type IA	1000	1000	1.18×10^{16}	1.143	9.33×10^{17}
Type IA	2.0×10^4	800	1.15×10^{16}	1.051	5.54×10^{17}
Type IB	2.0×10^4	800	1.55×10^{16}	1.774	1.04×10^{18}
Type IC	2.0×10^4	800	1.53×10^{16}	1.790	1.32×10^{18}

TABLE III: Mass scales in GeV unit and gauge couplings in the Type I $\mathcal{F} - SU(5)$ models for gauge coupling unification.

and M_U are respectively around 1.2×10^{16} GeV and 10^{17-18} GeV, and g_U is about 1.2. In Type IB and Type IC models, to avoid the Landau pole problem for gauge couplings, we choose $(M_V, M_S) = (20 \text{ TeV}, 800 \text{ GeV})$. We present the mass scales M_{23} and M_U , and the $SU(5) \times U(1)_X$ unified gauge couplings g_U in the Type I models in Table III. We find that M_{23} and M_U are respectively around 1.5×10^{16} GeV and 10^{18} GeV, and g_U is about 1.8. In Fig. 1, we plot the gauge coupling unification in the Type IA model with $M_V = 1 \text{ TeV}$ and $M_S = 800 \text{ GeV}$, and in the Type IB model with $M_V = 20 \text{ TeV}$ and $M_S = 800 \text{ GeV}$. Therefore, only the Type I models can be tested at the LHC since the universal mass for Z_1 set of vector-like particles can be below 1 TeV. We emphasize that the $SU(3)_C \times SU(2)_L$ unified coupling g_{23} (very close to g_U) is stronger than that in the traditional minimal

flipped $SU(5) \times U(1)_X$ models due to the TeV-scale vector-like particles, which will be very important in the proton decay as discussed in the Section VI [43].

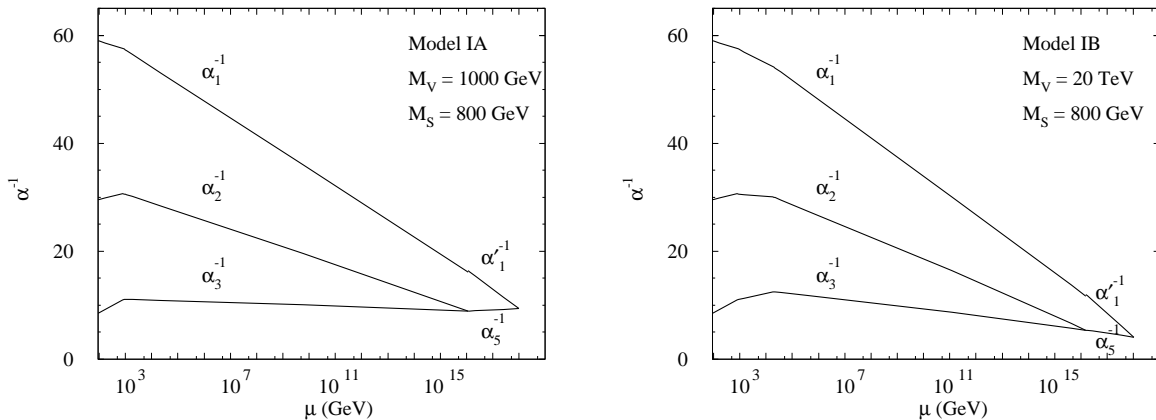


FIG. 1: Gauge coupling unification in the Type IA model with $M_V = 1$ TeV and $M_S = 800$ GeV (left figure), and in the Type IB model with $M_V = 20$ TeV and $M_S = 800$ GeV.

B. Type II Models with Intermediate-Scale Vector-Like Particles

In the Type II models, the one-loop contributions to the beta functions from the sets of vector-like particles satisfy $\Delta b_2 = \Delta b_3$ and $\Delta b_2 - \Delta b_1 = 12/5$. We consider two models. In the Type IIA model, we introduce Z_0 set of vector-like particles. And in the Type IIB model, we introduce Z_1 set of vector-like particles. Also, the curves with homology classes for the extra vector-like particles and the gauge bundle assignments for each curve in Type IIA and Type IIB models are given in Table II as well. For simplicity, we also assume that the masses for the vector-like particles are universal, and we denote the universal mass as M_V .

We study the gauge coupling unification in Type II models at the two-loop level. Note that $\Delta b_2 = \Delta b_3$ and $\Delta b_2 - \Delta b_1 = 12/5$, the $SU(5) \times U(1)_X$ unification scale M_U will be much higher than the Planck scale M_{Pl} if we put the Z_0 or Z_4 set of vector-like particles around the TeV scale, and then RGE running must include the supergravity corrections. Thus, we assume that M_V is at the intermediate scale so that we can avoid supergravity corrections to the RGE running. Choosing $M_S = 800$ GeV, and $M_V = 10^{10}$ GeV, 10^{11} GeV and 10^{12} GeV, we present the mass scales M_{23} and M_U , and the gauge couplings g_U in the Type II models in Table IV. To achieve the string-scale gauge coupling unification defined in Eq. 1, with $M_S = 800$ GeV, we obtain that M_V is equal to 3.68×10^{10} GeV in Type IIA model, and equal to 4.12×10^{10} GeV in Type IIB model. We present the corresponding mass scales and gauge couplings in Table IV as well. Moreover, we plot the string-scale gauge

Models	M_V	M_S	M_{23}	g_U	M_U
Type IIA	10^{10}	800	1.07×10^{16}	0.817	6.10×10^{16}
Type IIA	10^{11}	800	1.06×10^{16}	0.795	3.17×10^{17}
Type IIA	10^{12}	800	1.06×10^{16}	0.774	1.67×10^{17}
Type IIA	3.68×10^{10}	800	1.08×10^{16}	0.804	4.23×10^{17}
Type IIB	10^{10}	800	1.15×10^{16}	0.896	6.98×10^{17}
Type IIB	10^{11}	800	1.12×10^{16}	0.853	3.49×10^{17}
Type IIB	10^{12}	800	1.10×10^{16}	0.816	1.78×10^{17}
Type IIB	4.12×10^{10}	800	1.14×10^{16}	0.868	4.57×10^{17}

TABLE IV: Mass scales in GeV unit and gauge couplings in the Type II $\mathcal{F} - SU(5)$ models with gauge coupling unification and universal supersymmetry breaking.

coupling unification in the Type IIA and Type IIB models in Fig. 2. In short, we find that M_{23} and M_U are respectively around 1.1×10^{16} GeV and 10^{17} GeV, and g_U is about 0.8. Unfortunately, Type II models can not be tested at the LHC since the additional vector-like particles are at the intermediate scale.

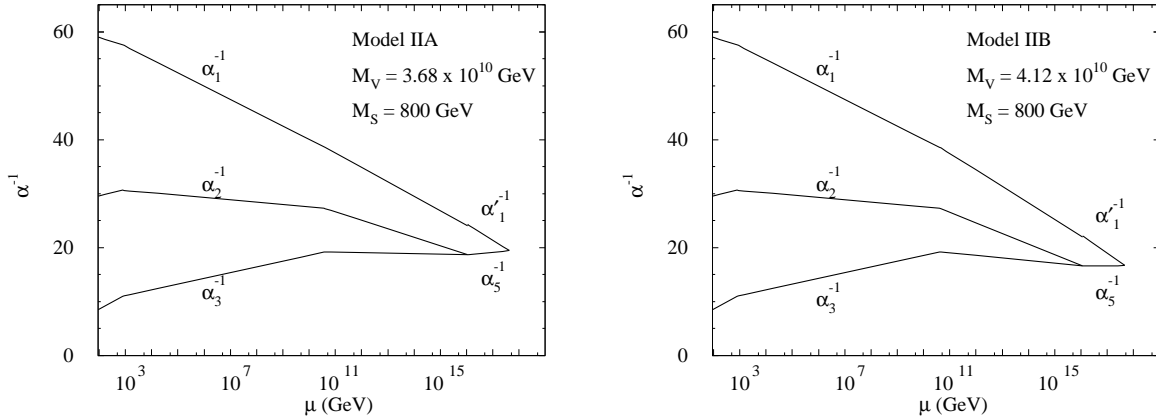


FIG. 2: String-scale gauge coupling unification in the Type IIA model (left figure) and Type IIB model (right figure) with $M_S = 800$ GeV.

C. Type III Models with the TeV-Scale and High-Scale Vector-Like Particles

In the Type III models, in addition to the vector-like particles around the TeV scale, we introduce the high-scale vector-like particles as well. For simplicity, we also assume that the masses of the high-scale vector-like particles are universal, and we denote their universal mass

as $M_{V'}$. In almost all of the Type III models, $M_{V'}$ is around the GUT scale or higher, so, the high-scale vector-like particles can be considered as the string-scale threshold corrections.

We consider four kinds of models. In the Type IIIA models, we introduce the following additional vector-like particles:

$$Z5 : XF + \overline{XF} + 3 \times (Xl_i + \overline{Xl}_i) , \quad (59)$$

where $i = 1, 2, 3$. In the Type IIIA1 model, we assume that the vector-like particles (XF, \overline{XF}) have masses around the TeV scale, while the vector-like particles (Xl_i, \overline{Xl}_i) with $i = 1, 2, 3$ have masses at the high scale. In the Type IIIA2 model, we assume that the vector-like particles (XF, \overline{XF}) and (Xl_1, \overline{Xl}_1) have masses around the TeV scale, while the vector-like particles (Xl_j, \overline{Xl}_j) with $j = 2, 3$ have masses at the high scale.

In the Type IIIB models, we introduce the following extra vector-like particles:

$$Z6 : XF + \overline{XF} + 4 \times (Xl_k + \overline{Xl}_k) , \quad (60)$$

where $k = 1, 2, 3, 4$. In the Type IIIB1 model, we assume that the vector-like particles (XF, \overline{XF}) have masses around the TeV scale, while the vector-like particles (Xl_k, \overline{Xl}_k) with $k = 1, 2, 3, 4$ have masses at the high scale. In the Type IIIB2 model, we assume that the vector-like particles (XF, \overline{XF}) and (Xl_4, \overline{Xl}_4) have masses around the TeV scale, while the vector-like particles (Xl_i, \overline{Xl}_i) with $i = 1, 2, 3$ have masses at the high scale.

In the Type IIIC models, we introduce the following additional vector-like particles:

$$Z7 : XF + \overline{XF} + 3 \times (Xl_i + \overline{Xl}_i) + Xf + \overline{Xf} , \quad (61)$$

where $i = 1, 2, 3$. In the Type IIIC1 model, we assume that the vector-like particles (XF, \overline{XF}) have masses around the TeV scale, while the vector-like particles (Xl_i, \overline{Xl}_i) with $i = 1, 2, 3$, and (Xf, \overline{Xf}) have masses at the high scale. In the Type IIIC2 model, we assume that the vector-like particles (XF, \overline{XF}) and (Xl_1, \overline{Xl}_1) have masses around the TeV scale, while the vector-like particles (Xl_j, \overline{Xl}_j) with $j = 2, 3$, and (Xf, \overline{Xf}) have masses at the high scale. In the Type IIIC3 model, we assume that the vector-like particles (XF, \overline{XF}) and (Xf, \overline{Xf}) have masses around the TeV scale, while the vector-like particles (Xl_i, \overline{Xl}_i) , with $i = 1, 2, 3$ have masses at the high scale.

In the Type IIID models, we introduce the following additional vector-like particles:

$$Z8 : XF + \overline{XF} + 3 \times (Xl_i + \overline{Xl}_i) + Xh + \overline{Xh} , \quad (62)$$

where $i = 1, 2, 3$. In the Type IIID1 model, we assume that the vector-like particles (XF, \overline{XF}) have masses around the TeV scale, while the vector-like particles (Xl_i, \overline{Xl}_i) with $i = 1, 2, 3$, and (Xh, \overline{Xh}) have masses at the high scale. In the Type IIID2 model, we

assume that the vector-like particles (XF, \overline{XF}) and (Xl_1, \overline{Xl}_1) have masses around the TeV scale, while the vector-like particles (Xl_j, \overline{Xl}_j) with $j = 2, 3$, and (Xh, \overline{Xh}) have masses at the high scale. In the Type IIID3 model, we assume that the vector-like particles (XF, \overline{XF}) and (Xh, \overline{Xh}) have masses around the TeV scale, while the vector-like particles (Xl_i, \overline{Xl}_i) with $i = 1, 2, 3$ have masses at the high scale. In the Type IIID4 model, we assume that the vector-like particles (XF, \overline{XF}) , (Xl_1, \overline{Xl}_1) and (Xh, \overline{Xh}) have masses around the TeV scale, while the vector-like particles (Xl_i, \overline{Xl}_i) with $i = 2, 3$ have masses at the high scale.

Models	Particles	Curve	Class	g_Σ	L_Σ	L_Σ^m
Type III	$(XF + \overline{XF})$	Σ_{XF} (pinched)	$3H - E_1 - E_2 - E_4$	1	$\mathcal{O}_{\Sigma_{XF}}(p_{12}^4)^{1/4}$	$\mathcal{O}_{\Sigma_{XF}}(p_{12}^4)^{-1/4}$
	$(Xl_i + \overline{Xl}_i)$	Σ_{Xl_i} (pinched)	$3H - E_1 - E_2 - E_j$	1	$\mathcal{O}_{\Sigma_{Xf}}(p_{12}^j)^{1/4}$	$\mathcal{O}_{\Sigma_{Xf}}(p_{12}^j)^{-5/4}$
Type IIIA	$(Xl + \overline{Xl})$	Σ_{Xl} (pinched)	$3H - E_1 - E_2 - E_5$	1	$\mathcal{O}_{\Sigma_{Xl}}(p_{12}^5)^{1/4}$	$\mathcal{O}_{\Sigma_{Xf}}(p_{12}^5)^{-5/4}$
Type IIIB	$(Xf + \overline{Xf})$	Σ_{Xf} (pinched)	$3H - E_1 - E_2 - E_5$	1	$\mathcal{O}_{\Sigma_{Xf}}(p_{12}^5)^{1/4}$	$\mathcal{O}_{\Sigma_{Xf}}(p_{12}^5)^{3/4}$
Type IIID	$(Xh + \overline{Xh})$	Σ_{Xh} (pinched)	$3H - E_1 - E_2 - E_5$	1	$\mathcal{O}_{\Sigma_{Xh}}(p_{12}^5)^{1/4}$	$\mathcal{O}_{\Sigma_{Xh}}(p_{12}^5)^{1/2}$

TABLE V: The vector-like particle curves and the gauge bundle assignments for each curve in Type III models. In particular, we have the vector-like particles (XF, \overline{XF}) and (Xl_i, \overline{Xl}_i) with $i = 1, 2, 3$ in all the Type III models. Here, $j = i + 5$, and $p_{12}^m = p_1^m - p_2^m$ for $m = 4, 5, 6, 7, 8$. And we denote the corresponding blowing up points as p_1^m or p_2^m .

Moreover, the curves with homology classes for the additional vector-like particles and the gauge bundle assignments for each curve in Type III models are given in Table V. We also present the complete additional vector-like particles at the scales M_V and $M_{V'}$ in Type III models in the Table VI. In short, at the TeV scale, we have $Z0$ set of vector-like particles in the Type IIIX1 models where $X=A, B, C, D$; we have $Z1$ set of vector-like particles in the Type IIIX2 models; we have $Z2$ set of vector-like particles in the Type IIIC3 model; we have $Z3$ set of vector-like particles in the Type IIID4 model; and we have $Z4$ set of vector-like particles in the Type IIID3 model.

Furthermore, first, we study the gauge coupling unification in Type III models at the two-loop level. We choose $M_S = 800$ GeV and $M_{V'} = 1 \times 10^{16}$ GeV. For the Type IIIX1 and Type IIIX2 models, we choose $M_V = 1$ TeV. To avoid the Landau pole problem for gauge couplings, we choose $M_V = 5$ TeV in the Type IIIC3 and Type IIID4 models, and choose $M_V = 50$ TeV in the Type IIID3 model. We present the mass scales M_{23} and M_U , and the gauge couplings g_U in the Type III models in Table VII. Moreover, we find that M_{23} and M_U are respectively around 1.4×10^{16} GeV and 10^{17-18} GeV. Also, g_U is about 1.2 in the Type IIIX1 and Type IIIX2 models, 1.6 in the Type IIID3 model, 2.47 in the Type

Models	Particles at M_V	Particles at $M_{V'}$
Type IIIA1	(XF, \overline{XF})	(Xl_i, \overline{Xl}_i) for $i = 1, 2, 3$
Type IIIA2	$(XF, \overline{XF}), (Xl_1, \overline{Xl}_1)$	(Xl_j, \overline{Xl}_j) for $j = 2, 3$
Type IIIB1	(XF, \overline{XF})	(Xl_k, \overline{Xl}_k) for $k = 1, 2, 3, 4$
Type IIIB2	$(XF, \overline{XF}), (Xl_4, \overline{Xl}_4)$	(Xl_i, \overline{Xl}_i) for $i = 1, 2, 3$
Type IIIC1	(XF, \overline{XF})	(Xl_i, \overline{Xl}_i) for $i = 1, 2, 3, (Xf, \overline{Xf})$
Type IIIC2	$(XF, \overline{XF}), (Xl_1, \overline{Xl}_1)$	(Xl_j, \overline{Xl}_j) for $j = 2, 3, (Xf, \overline{Xf})$
Type IIIC3	$(XF, \overline{XF}), (Xf, \overline{Xf})$	(Xl_i, \overline{Xl}_i) for $i = 1, 2, 3$
Type IIID1	(XF, \overline{XF})	(Xl_i, \overline{Xl}_i) for $i = 1, 2, 3, (Xh, \overline{Xh})$
Type IIID2	$(XF, \overline{XF}), (Xl_1, \overline{Xl}_1)$	(Xl_j, \overline{Xl}_j) for $j = 2, 3, (Xh, \overline{Xh})$
Type IIID3	$(XF, \overline{XF}), (Xh, \overline{Xh})$	(Xl_i, \overline{Xl}_i) for $i = 1, 2, 3$
Type IIID4	$(XF, \overline{XF}), (Xl_1, \overline{Xl}_1), (Xh, \overline{Xh})$	(Xl_j, \overline{Xl}_j) for $j = 2, 3$

TABLE VI: The additional vector-like particles at the scales M_V and $M_{V'}$, where $i = 1, 2, 3$, $j = 2, 3$, $k = 1, 2, 3, 4$.

IIIC3 model, and 3.39 in the Type IIID4 model. Thus, the unified couplings in the Type IIIC3 and Type IIID4 models are strong.

Second, we study the string-scale gauge coupling unification in Type III models at the two-loop level, and the mass scales $M_{V'}$ are determined from the condition for string-scale gauge coupling unification given in Eq. 1. We also choose $M_S = 800$ GeV. For the Type IIIX1 and Type IIIX2 models, we choose $M_V = 1$ TeV. To avoid the Landau pole problem for gauge couplings, we choose $M_V = 10$ TeV in the Type IIIC3 and Type IIID4 models, and $M_V = 50$ TeV in the Type IIID3 model. We present the mass scales M_{23} and M_{string} , and the gauge couplings g_{string} in the Type III models in Table VIII. In Fig. 3, we plot the string-scale gauge coupling unification in the Type IIIB1 and Type IIIB2 models with $M_V = 1$ TeV and $M_S = 800$ GeV. Moreover, we find that M_{23} and M_{string} are respectively around 1.4×10^{16} GeV and 10^{17-18} GeV. Also, g_{string} is about 1.2 in the Type IIIX1 and Type IIIX2 models, about 1.5 in the Type IIID3 model, and about 2.1 in the Type IIIC3 and Type IIID4 models. In addition, in the Type IIIX2, Type IIIC3 and Type IIID4 models, the high-scale vector-like particles can be considered as string-scale threshold corrections since their masses are about 10^{17} GeV. While in the Type IIIX1 and Type IIID3 models, the masses for the vector-like particles are at the intermediate scale 10^{12-13} GeV.

Models	M_V	M_S	M_{23}	$M_{V'}$	g_U	M_U
Type IIIA1	1000	800	1.17×10^{16}	1×10^{16}	1.142	7.22×10^{18}
Type IIIA2	1000	800	1.17×10^{16}	1×10^{16}	1.161	4.05×10^{17}
Type IIIB1	1000	800	1.17×10^{16}	1×10^{16}	1.145	4.04×10^{18}
Type IIIB2	1000	800	1.17×10^{16}	1×10^{16}	1.163	2.92×10^{17}
Type IIIC1	1000	800	1.17×10^{16}	1×10^{16}	1.226	4.11×10^{18}
Type IIIC2	1000	800	1.18×10^{16}	1×10^{16}	1.207	2.93×10^{17}
Type IIIC3	5000	800	1.72×10^{16}	1×10^{16}	2.470	4.41×10^{17}
Type IIID1	1000	800	1.17×10^{16}	1×10^{16}	1.231	7.77×10^{18}
Type IIID2	1000	800	1.17×10^{16}	1×10^{16}	1.209	4.19×10^{17}
Type IIID3	5.0×10^4	800	1.50×10^{16}	1×10^{16}	1.613	5.19×10^{18}
Type IIID4	5000	800	1.69×10^{16}	1×10^{16}	3.390	9.97×10^{17}

TABLE VII: Mass scales in GeV unit and gauge couplings in the Type III $\mathcal{F} - SU(5)$ models with gauge coupling unification and universal supersymmetry breaking.

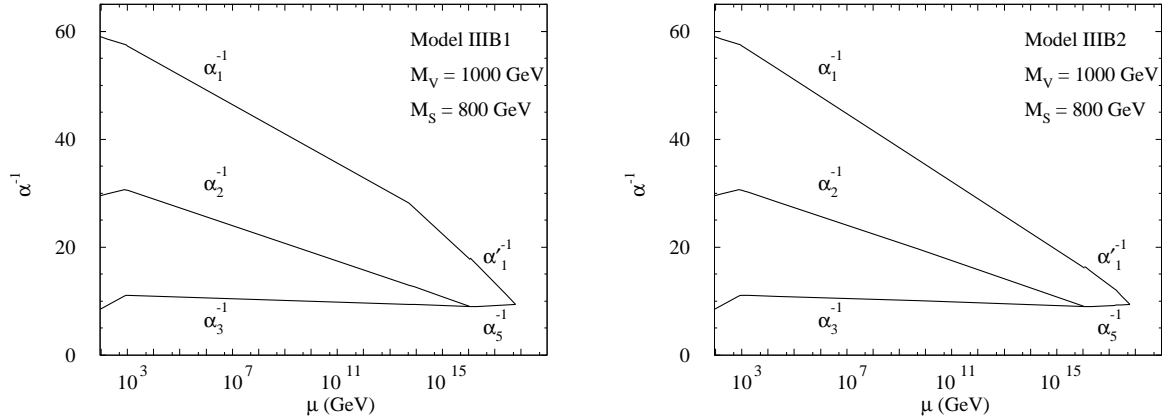


FIG. 3: String-scale gauge coupling unification in the Type IIIB1 model (left figure) and Type IIIB2 model (right figure) with $M_V = 1$ TeV and $M_S = 800$ GeV.

V. FLIPPED $SU(5) \times U(1)_X$ MODELS WITH BULK VECTOR-LIKE PARTICLES

In all the above flipped $SU(5) \times U(1)_X$ models, we can introduce the bulk vector-like particles XT_i and \overline{XT}_i on the observable seven-branes as well. If we choose the line bundle $L = \mathcal{O}_S(E_1 - E_2 + E_4 - E_5)^{1/4}$, we have one pair of the bulk vector-like particles XT_1 and \overline{XT}_1 on the surface S since $\chi(S, L^4)$ is equal to -1 . And if we choose the line bundle $L = \mathcal{O}_S(E_1 - E_2 + E_4 - E_5 + E_6 - E_7)^{1/4}$, we have two pairs of the bulk vector-like particles XT_i and \overline{XT}_i on the surface S since $\chi(S, L^4)$ is equal to -2 . For the Type I, Type II and Type

Models	M_V	M_S	M_{23}	$M_{V'}$	g_{string}	M_{string}
Type IIIA1	1000	800	1.13×10^{16}	2.04×10^{12}	1.161	6.12×10^{17}
Type IIIA2	1000	800	1.18×10^{16}	8.32×10^{16}	1.158	6.10×10^{17}
Type IIIB1	1000	800	1.13×10^{16}	4.79×10^{12}	1.161	6.12×10^{17}
Type IIIB2	1000	800	1.18×10^{16}	1.62×10^{17}	1.158	6.10×10^{17}
Type IIIC1	1000	800	1.20×10^{16}	5.67×10^{12}	1.302	6.86×10^{17}
Type IIIC2	1000	800	1.18×10^{16}	1.70×10^{17}	1.174	6.18×10^{17}
Type IIIC3	1×10^4	800	1.65×10^{16}	5.64×10^{17}	2.087	1.10×10^{18}
Type IIID1	1000	800	1.24×10^{16}	1.92×10^{12}	1.375	7.25×10^{17}
Type IIID2	1000	800	1.18×10^{16}	8.55×10^{16}	1.182	6.23×10^{17}
Type IIID3	5×10^4	800	1.50×10^{16}	2.38×10^{13}	1.533	8.08×10^{17}
Type IIID4	1×10^4	800	1.62×10^{16}	1.46×10^{17}	2.074	1.09×10^{18}

TABLE VIII: Mass scales in GeV unit and gauge couplings in the Type III $\mathcal{F} - SU(5)$ models with string-scale gauge coupling unification and universal supersymmetry breaking.

III models with one pair and two pairs of the bulk vector-like particles XT_i and \overline{XT}_i , we present the curves with homology classes for the vector-like particles, and the gauge bundle assignments for each curve in Appendices B and C, respectively. Moreover, the vector-like particles XT_i and \overline{XT}_i can obtain masses via instanton effects. Also, they can couple to the singlets from the intersections of the other seven-branes, and then obtain masses from Higgs mechanism. Thus, the vector-like particles XT_i and \overline{XT}_i can have masses $M_{V'}$ close to the string scale (or intermediate scale) and can be considered as the string-scale (or intermediate scale) threshold corrections.

To avoid the Landau pole problem for the gauge couplings, we have shown that only the Z_0 and Z_1 sets of vector-like particles can be below 1 TeV, which can be tested at the LHC. Thus, in this Section, we will concentrate on the Type IA and Type IIA models with bulk vector-like particles XT_i and \overline{XT}_i . In the Type IA1 and Type IIA1 models, we introduce one pair of vector-like particles XT_1 and \overline{XT}_1 . Also, in the Type IA2 and Type IIA2 models, we introduce two pairs of vector-like particles XT_i and \overline{XT}_i with $i = 1, 2$. The particle contents of these models are given in Table IX.

We give the one-loop and two-loop beta functions for XT_i and \overline{XT}_i in the supersymmetric Standard Model and in the flipped $SU(5) \times U(1)_X$ model in the Appendix D. First, we study the gauge coupling unification at the two-loop level. Choosing $M_V = 800$ GeV, $M_S = 800$ GeV, and $M_{V'} = 1 \times 10^{16}$ GeV, we present the mass scales M_{23} and M_U , and the gauge couplings g_U in Table X. In these models, M_{23} and M_U are respectively around

Models	Particles at M_V	Particles at $M_{V'}$
Type IA1	$(XF, \overline{XF}), (Xl, \overline{Xl})$	(XT_1, \overline{XT}_1)
Type IA2	$(XF, \overline{XF}), (Xl, \overline{Xl})$	(XT_i, \overline{XT}_i) for $i = 1, 2$
Type IIA1	(XF, \overline{XF})	(XT_1, \overline{XT}_1)
Type IIA2	(XF, \overline{XF})	(XT_i, \overline{XT}_i) for $i = 1, 2$

TABLE IX: The particle contents in the Type IA1, Type IA2, Type IIA1 and Type IIA2 models.

Models	M_V	M_S	M_{23}	$M_{V'}$	g_U	M_U
Type IA1	800	800	1.18×10^{16}	1×10^{16}	1.322	2.16×10^{17}
Type IA2	800	800	1.18×10^{16}	1×10^{16}	1.428	9.85×10^{16}
Type IIA1	800	800	1.18×10^{16}	1×10^{16}	1.527	3.87×10^{18}
Type IIA2	800	800	1.18×10^{16}	1×10^{16}	1.996	7.53×10^{17}

TABLE X: Mass scales in GeV unit and gauge couplings in Type IA1, Type IA2, Type IIA1 and Type IIA2 models with gauge coupling unification and universal supersymmetry breaking.

1.2×10^{16} GeV and 10^{17-18} GeV, and g_U is about 1.4 in the Type IA1, Type IA2 and Type IIA1 models, and about 2.0 in the Type IIA2 model. Because the Type IA1 (IIA1) and Type IA2 (IIA2) models respectively have one pair and two pairs of vector-like particles XT_i and \overline{XT}_i , the unified coupling g_U in the Type IA1 (IIA1) model is smaller than that in the Type IA2 (IIA2) model while M_U in the Type IA1 (IIA1) model is larger than that in

Models	M_V	M_S	M_{23}	$M_{V'}$	g_{string}	M_{string}
Type IA1	800	800	1.18×10^{16}	2.46×10^{17}	1.205	6.35×10^{17}
Type IA2	800	800	1.18×10^{16}	3.95×10^{17}	1.205	6.35×10^{17}
Type IIA1	800	800	1.20×10^{16}	2.04×10^{14}	2.020	1.06×10^{18}
Type IIA2	200	360	1.21×10^{16}	4.42×10^{16}	4.288	2.26×10^{18}
Type IIA2	200	1000	1.25×10^{16}	1.70×10^{16}	2.153	1.13×10^{18}
Type IIA2	1000	360	1.17×10^{16}	1.91×10^{16}	2.142	1.13×10^{18}
Type IIA2	1000	1000	1.18×10^{16}	1.65×10^{16}	1.862	9.81×10^{17}

TABLE XI: Mass scales in GeV unit and gauge couplings in the Type IA1, Type IA2, Type IIA1 and Type IIA2 models with string-scale gauge coupling unification and universal supersymmetry breaking.

the Type IA2 (IIA2) model.

Second, we study the string-scale gauge coupling unification at the two-loop level, and the mass scales $M_{V'}$ are determined from the condition for string-scale gauge coupling unification given in Eq. 1. In the Type IA1, Type IA2, and Type IIA2 models, we choose $M_V = 800$ GeV and $M_S = 800$ GeV. In the Type IIA2 model, we choose $(M_V, M_S) = (200$ GeV, 360 GeV), (200 GeV, 1000 GeV), (1000 GeV, 360 GeV), and (1000 GeV, 1000 GeV). We present the mass scales M_{23} and M_{string} , and the gauge couplings g_{string} in Table XI. In the Fig. 4, we present the string-scale gauge coupling unification in the Type IIA1 model with $M_V = 800$ GeV and $M_S = 800$ GeV, and in the Type IIA2 model with $M_V = 1$ TeV and $M_S = 800$ GeV. We find that M_{23} is about 1.2×10^{16} GeV in all the models. In the Type IA1 and Type IA2 models, M_{string} is about 6.35×10^{17} GeV, and g_{string} is about 1.2. In the Type IIA1 and Type IIA2 models, M_{string} is about 1.0×10^{18} GeV, and g_{string} is about 2.0 or larger. In addition, in the Type IA1, Type IA2 and Type IIA2 models, the bulk vector-like particles can be considered as string-scale threshold corrections since their masses are about 10^{16-17} GeV. While in the Type IIA1 model, the masses for the bulk vector-like particles are at the intermediate scale 10^{14} GeV.

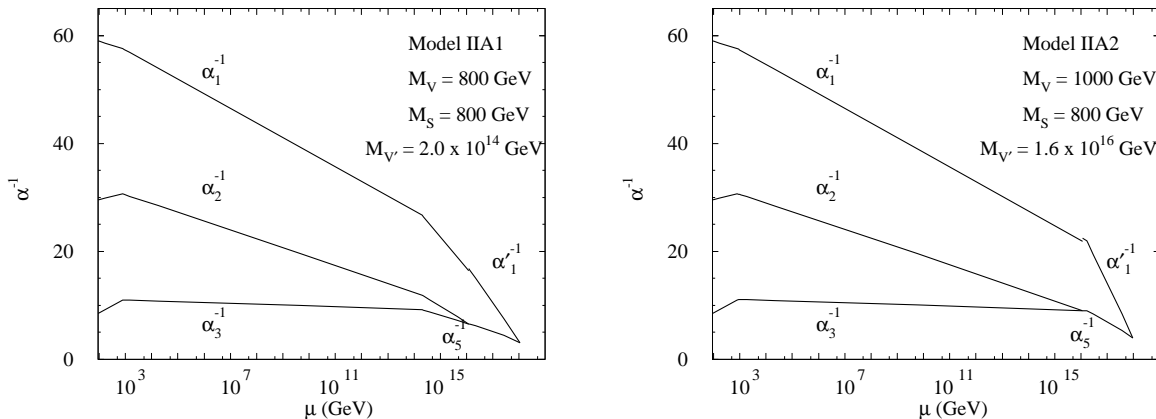


FIG. 4: The string-scale gauge coupling unification in the Type IIA1 model with $M_V = 800$ GeV and $M_S = 800$ GeV (left figure) and in the Type IIA2 model with $M_V = 1$ TeV and $M_S = 800$ GeV (right figure).

VI. PHENOMENOLOGICAL CONSEQUENCES

In this Section, we will discuss the phenomenological consequences in our models. Similar to the minimal flipped $SU(5) \times U(1)_X$ models, the doublet-triplet splitting problem can be solved in all of our models in general. Let us comment on the phenomenological consequences one by one in the following:

(i) Because GUTs in F-theory are constructed locally, we may have additional chiral exotic particles or vector-like particles when we embed such F-theory GUTs into the global consistent setup. The point is that there may exist additional seven-branes due to the global consistent conditions, and these seven-branes may intersect with the observable seven-branes.

(ii) In the Type IA and Type III_X2 models where X=A, B, C, D, we can have Z_1 set of vector-like particles below the 1 TeV scale. Also, in the Type IIA models with bulk vector-like particles and in the Type III_X1 models, we have Z_0 set of vector-like particles below the 1 TeV scale. Thus, these Z_1 and Z_0 sets of vector-like particles can be produced at the LHC, and then the corresponding models can be tested. Moreover, at the low energy, in the Type IB and Type III_C3 models, we have Z_2 set of vector-like particles; in the Type IC and Type III_D4 models, we have Z_3 set of vector-like particles; and in the Type IIB models with bulk vector-like particles and the Type III_D3 model, we have Z_4 set of vector-like particles. The masses for the Z_2 , Z_3 , or Z_4 set of vector-like particles in these models are around 10 TeV. Because of the threshold corrections at the scales M_{SUSY} and M_{23} , the masses of these vector-like particles might be around the 1 TeV scale, and then these models could be tested at the LHC as well. Therefore, all of our models with Z_0 , Z_1 , Z_2 , Z_3 , or Z_4 set of vector-like particles at the TeV scale might be tested at the LHC. The detail study will be presented elsewhere [67].

(iii) It is well known that the lightest CP-even Higgs boson mass in the MSSM is smaller than about 130 GeV if M_S is smaller than 1 TeV, which is a several percents' fine-tuning problem in the MSSM. In all our models with TeV-scale vector-like particles, we have the vector-like particles XF and \overline{XF} . Then we can introduce the following Yukawa interactions between the MSSM Higgs fields and these vector-like particles in the flipped $SU(5) \times U(1)_X$ models:

$$-\mathcal{L} = y_{XF}^d XF XF h + y_{XF}^u \overline{XF} \overline{XF} h, \quad (63)$$

where y_{XF}^d and y_{XF}^u are Yukawa couplings. With relatively large Yukawa couplings y_{XF}^d and y_{XF}^u that are consistent with the perturbative unification, we can increase the lightest CP-even Higgs boson mass and solve the Higgs mass problem in the MSSM [67, 68].

(iv) The proton decay via dimension-5 operators from Higgsino exchange is suppressed. Considering proton decay $p \rightarrow e^+ \pi^0$ via dimension-6 operator from heavy gauge boson exchange, we obtain the proton life time [43, 69]

$$\tau_p \simeq 9.97 \times 10^{34} \left(\frac{M_{23}}{1.18 \times 10^{16} \text{GeV}} \right)^4 \left(\frac{1.193}{g_{23}} \right)^4 \text{ yr}, \quad (64)$$

where g_{23} is the $SU(3)_C \times SU(2)_L$ unified gauge coupling. In all of our models with TeV-scale vector-like particles (the Type I and Type III models, and Type II models with bulk

vector-like particles), g_{23} is about 1.2 or larger. In addition, M_{23} can be another factor 2/3 smaller due to threshold corrections [69], thus, our models can definitely be tested at the future Hyper-Kamiokande proton decay experiment which can search the proton life time via $p \rightarrow e^+\pi^0$ channel at least more than 10^{35} years [63]. Similar results can be applied to the F-theory $SU(5)$ models with vector-like particles. Our systematical and comprehensive study will be presented elsewhere [70]. By the way, the Kaluza-Klein modes of the gauge bosons could further enhance the proton decay. However, the details depend on the estimations of the bulk Green's functions for the gauge bosons which have some unknown constants [32].

(v) From Eq. (11), we obtain that the neutrino masses and mixings can be explained via double seesaw mechanism [71]. Also, the right-handed neutrino Majorana masses can be generated via the following dimension-5 operators after we integrate out the heavy Kaluza-Klein modes [33, 34]

$$W = \frac{y_{ij}^{iN}}{M_U} F_i F_j \overline{H} H . \quad (65)$$

So the neutrino masses and mixings can be generated via seesaw mechanism as well. With leptogenesis [72], we can obtain the observed baryon asymmetry [71].

(vi) From Eq. (10), we can naturally have the hybrid inflation where Φ is the inflaton field [73]. The inflation scale is related to the scale M_{23} . Because M_{23} is at least one order smaller than M_U , we solve the monopole problem. Interestingly, we can generate the correct cosmic primordial density fluctuations [74]

$$\frac{\delta\rho}{\rho} \sim \left(\frac{M_{23}}{g_{23} M_{\text{Pl}}} \right)^2 \sim 1.7 \times 10^{-5} . \quad (66)$$

Therefore, the key question is whether we can generate $\Phi(\overline{H}H - M_H^2)$ terms in Eq. (10). Our detail study will be given elsewhere [75]. Here let us briefly sketch the idea. Let us suppose that the H and \overline{H} arise from the intersection of the observable seven-branes and the seven-brane that wraps a complex codimension-one surface S_H in B_3 , and Φ arises from the intersection between the seven-brane wrapping S_H and the seven-brane that wraps a complex codimension-one surface S_Φ in B_3 . Because the curve Σ_H is self pinched, we have the trilinear superpotential $\Phi\overline{H}H$ if the curve on which Φ is localized passes the pinched point in B_3 . In addition, the term $M_H^2\Phi$ can be generated via instanton effects [36]. Assume that the volumes for S_H and S_Φ are the same and their compactification scale is M_{C2} , we obtain

$$M_H \simeq M_U \exp \left(-\frac{4\pi^2}{g_U^2} \frac{M_U^4}{M_{C2}^4} \right) . \quad (67)$$

Without fine-tuning, we can choose $M_{C2} = 2M_U$, and then we can obtain the correct scale for M_H .

VII. DISCUSSION AND CONCLUSIONS

In this paper, we briefly reviewed the flipped $SU(5) \times U(1)$ models and the F-theory model building. To separate the mass scales M_{23} and M_U and realize the decoupling scenario, we introduced sets of vector-like particles in complete $SU(5) \times U(1)$ multiplets at the low energy, whose one-loop beta functions satisfy $\Delta b_1 < \Delta b_2 = \Delta b_3$. To avoid the Landau pole problem for the gauge couplings, we can only introduce five sets of such vector-like particles around the TeV scale. Moreover, we have systematically constructed the flipped $SU(5) \times U(1)_X$ models without bulk vector-like particles, and the flipped $SU(5) \times U(1)_X$ models with bulk vector-like particles. These vector-like particles can couple to the SM singlet fields, and obtain suitable masses through Higgs mechanism. In addition, we considered the gauge coupling unification in all of our models without bulk vector-like particles, and in the Type IA and Type IIA models with bulk vector-like particles. We also studied the string-scale gauge coupling unification in the Type III models, and the Type IA and Type IIA models with bulk vector-like particles. We showed that the $U(1)_X$ flux contributions to the gauge couplings preserve the $SU(5) \times U(1)_X$ gauge coupling unification. We calculated the mass scales M_{23} and M_U , and the unified couplings g_U . In the Type IIIX2, Type IIIC3, Type IIID4, Type IA1, Type IA2, and Type IIA2 models, the high-scale or bulk vector-like particles can be considered as string-scale threshold corrections since their masses are close to the string scale. We showed that the Z_0 and Z_1 sets of vector-like particles can have masses below the 1 TeV scale, and then they can be observed at the LHC. Thus, the corresponding models, which have Z_0 or Z_1 sets of vector-like particles at about 1 TeV scale, can be tested at the LHC.

Furthermore, we discussed the phenomenological consequences of our models. We pointed out that there may exist additional chiral exotic particles or vector-like particles when we embed our models into the global consistent setup. Due to the threshold corrections at the scales M_S and M_{23} , the Z_2 , Z_3 , and Z_4 sets of vector-like particles might also have masses below the 1 TeV scale, and then the corresponding models with such sets could be tested at the LHC as well. In all our models with TeV-scale vector-like particles, the proton decay is within the reach of the future Hyper-Kamiokande experiment, the lightest CP-even Higgs boson mass can be increased due to the Yukawa couplings between the Higgs fields and TeV-scale vector-like particles, the neutrino masses and mixings can be explained via the double seesaw or seesaw mechanism, the observed baryon asymmetry can be obtained through leptogenesis, the hybrid inflation can be realized, the monopole problem can be solved, and the correct cosmic primordial density fluctuations can be generated.

Acknowledgments

This research was supported in part by the Cambridge-Mitchell Collaboration in Theoretical Cosmology (TL), by the Natural Science Foundation of China under grant No. 10821504 (TL), and by the DOE grant DE-FG03-95-Er-40917 (DVN).

Appendix A: Briefly Review of del Pezzo Surfaces

The del Pezzo surfaces dP_n , where $n = 1, 2, \dots, 8$, are defined by blowing up n generic points of $\mathbb{P}^1 \times \mathbb{P}^1$ or \mathbb{P}^2 . The homological group $H_2(dP_n, Z)$ has the generators

$$H, E_1, E_2, \dots, E_n, \quad (\text{A1})$$

where H is the hyperplane class for P^2 , and E_i are the exceptional divisors at the blowing up points and are isomorphic to \mathbb{P}^1 . The intersecting numbers of the generators are

$$H \cdot H = 1, \quad E_i \cdot E_j = -\delta_{ij}, \quad H \cdot E_i = 0. \quad (\text{A2})$$

The canonical bundle on dP_n is given by

$$K_{dP_n} = -c_1(dP_n) = -3H + \sum_{i=1}^n E_i. \quad (\text{A3})$$

For $n \geq 3$, we can define the generators as follows

$$\alpha_i = E_i - E_{i+1}, \quad \text{where } i = 1, 2, \dots, n-1, \quad (\text{A4})$$

$$\alpha_n = H - E_1 - E_2 - E_3. \quad (\text{A5})$$

Thus, all the generators α_i is perpendicular to the canonical class K_{dP_n} . And the intersection products are equal to the negative Cartan matrix of the Lie algebra E_n , and can be considered as simple roots.

The curves Σ_i in dP_n where the particles are localized must be divisors of S . And the genus for curve Σ_i is given by

$$2g_i - 2 = [\Sigma_i] \cdot ([\Sigma_i] + K_{dP_k}). \quad (\text{A6})$$

For a line bundle L on the surface dP_n with

$$c_1(L) = \sum_{i=1}^n a_i E_i, \quad (\text{A7})$$

where $a_i a_j < 0$ for some $i \neq j$, the Kähler form J_{dP_n} can be constructed as follows [33]

$$J_{dP_k} = b_0 H - \sum_{i=1}^n b_i E_i, \quad (\text{A8})$$

where $\sum_{i=1}^k a_i b_i = 0$ and $b_0 \gg b_i > 0$. By the construction, it is easy to see that the line bundle L solves the BPS equation $J_{dP_k} \wedge c_1(L) = 0$.

Appendix B: The Vector-Like Particle Curves and the Gauge Bundle Assignments in the Models with One Pair of the Bulk Vector-Like Particles

In the Type I, Type II, and Type III models, we can introduce one pair of the bulk vector-like particles XT_1 and \overline{XT}_1 . Let us choose the line bundle $L = \mathcal{O}_S(E_1 - E_2 + E_4 - E_5)^{1/4}$. Note that $\chi(S, L^4)$ is equal to -1 , we have one pair of the bulk vector-like particles XT_1 and \overline{XT}_1 . We present the curves with homology classes for the vector-like particles, and the gauge bundle assignments for each curve in the corresponding Type I and Type II models in Table XII, and in the corresponding Type III models in Table XIII.

Model	Particles	Curve	Class	g_Σ	L_Σ	L_Σ^m
Type I & II	$(XF + \overline{XF})$	Σ_{XF} (pinched)	$3H - E_4 - E_5$	1	$\mathcal{O}_{\Sigma_{XF}}(p_{45})^{1/4}$	$\mathcal{O}_{\Sigma_{XF}}(p_{45})^{-1/4}$
Type IA	$(Xl + \overline{Xl})$	Σ_{Xl} (pinched)	$3H - E_1 - E_5$	1	$\mathcal{O}_{\Sigma_{Xl}}(p'_{15})^{1/4}$	$\mathcal{O}_{\Sigma_{Xl}}(p'_{15})^{-5/4}$
Type IB	$(Xf + \overline{Xf})$	Σ_{Xf} (pinched)	$3H - E_1 - E_5$	1	$\mathcal{O}_{\Sigma_{Xf}}(p'_{15})^{1/4}$	$\mathcal{O}_{\Sigma_{Xl}}(p'_{15})^{3/4}$
Type IC	$(Xl + \overline{Xl})$	Σ_{Xl} (pinched)	$3H - E_1 - E_5$	1	$\mathcal{O}_{\Sigma_{Xl}}(p'_{15})^{1/4}$	$\mathcal{O}_{\Sigma_{Xl}}(p'_{15})^{-5/4}$
	$(Xh + \overline{Xh})$	Σ_{Xh} (pinched)	$3H - E_2 - E_4$	1	$\mathcal{O}_{\Sigma_{Xh}}(p'_{42})^{1/4}$	$\mathcal{O}_{\Sigma_{Xh}}(p'_{42})^{1/2}$
Type IIB	$(Xh + \overline{Xh})$	Σ_{Xh} (pinched)	$3H - E_1 - E_5$	1	$\mathcal{O}_{\Sigma_{Xh}}(p'_{15})^{1/4}$	$\mathcal{O}_{\Sigma_{Xh}}(p'_{15})^{1/2}$

TABLE XII: The vector-like particle curves and the gauge bundle assignments for each curve in Type I and Type II models with one pair of bulk vector-like particles (XT_1 and \overline{XT}_1). Here, $p_{45} = p_4 - p_5$, $p'_{15} = p'_1 - p'_5$, and $p'_{42} = p'_4 - p'_2$.

Models	Particles	Curve	Class	g_Σ	L_Σ	L_Σ^m
Type III	$(XF + \overline{XF})$	Σ_{XF} (pinched)	$3H - E_4 - E_5$	1	$\mathcal{O}_{\Sigma_{XF}}(p_{45})^{1/4}$	$\mathcal{O}_{\Sigma_{XF}}(p_{45})^{-1/4}$
	$(Xl_i + \overline{Xl}_i)$	Σ_{Xl_i} (pinched)	$3H - E_1 - E_2 - E_j$	1	$\mathcal{O}_{\Sigma_{Xf}}(p'_{12})^{1/4}$	$\mathcal{O}_{\Sigma_{Xf}}(p'_{12})^{-5/4}$
Type IIIA	$(Xl + \overline{Xl})$	Σ_{Xl} (pinched)	$3H - E_1 - E_5$	1	$\mathcal{O}_{\Sigma_{Xl}}(p'_{15})^{1/4}$	$\mathcal{O}_{\Sigma_{Xf}}(p'_{15})^{-5/4}$
Type IIIB	$(Xf + \overline{Xf})$	Σ_{Xf} (pinched)	$3H - E_1 - E_5$	1	$\mathcal{O}_{\Sigma_{Xf}}(p'_{15})^{1/4}$	$\mathcal{O}_{\Sigma_{Xf}}(p'_{15})^{3/4}$
Type IIID	$(Xh + \overline{Xh})$	Σ_{Xh} (pinched)	$3H - E_1 - E_5$	1	$\mathcal{O}_{\Sigma_{Xh}}(p'_{15})^{1/4}$	$\mathcal{O}_{\Sigma_{Xh}}(p'_{15})^{1/2}$

TABLE XIII: The vector-like particle curves and the gauge bundle assignments for each curve in Type IIIA models with one pair of bulk vector-like particles (XT_1 and \overline{XT}_1). Here, $p_{45} = p_4 - p_5$, $p'_{15} = p'_1 - p'_5$, $j = i + 5$, and $p'_{12} = p'_1 - p'_2$ for $j = 6, 7, 8$.

Appendix C: The Vector-Like Particle Curves and the Gauge Bundle Assignments in the Models with Two Pairs of the Bulk Vector-Like Particles

In the Type I, Type II, and Type III models, we can also introduce two pairs of the bulk vector-like particles XT_i and \overline{XT}_i . Let us choose the line bundle $L = \mathcal{O}_S(E_1 - E_2 + E_4 - E_5 + E_6 - E_7)^{1/4}$. Note that $\chi(S, L^4)$ is equal to -2 , we have two pairs of the bulk vector-like particles XT_i and \overline{XT}_i . We present the curves with homology classes for the vector-like particles, and the gauge bundle assignments for each curve in the corresponding Type I and Type II models in Table XIV, and in the corresponding Type III models in Table XV.

Model	Particles	Curve	Class	g_Σ	L_Σ	L_Σ^n
Type I & II	$(XF + \overline{XF})$	Σ_{XF} (pinched)	$3H - E_4 - E_5$	1	$\mathcal{O}_{\Sigma_{XF}}(p_{45})^{1/4}$	$\mathcal{O}_{\Sigma_{XF}}(p_{45})^{-1/4}$
Type IA	$(Xl + \overline{Xl})$	Σ_{Xl} (pinched)	$3H - E_6 - E_7$	1	$\mathcal{O}_{\Sigma_{Xl}}(p_{67})^{1/4}$	$\mathcal{O}_{\Sigma_{Xl}}(p_{67})^{-5/4}$
Type IB	$(Xf + \overline{Xf})$	Σ_{Xf} (pinched)	$3H - E_6 - E_7$	1	$\mathcal{O}_{\Sigma_{Xf}}(p_{67})^{1/4}$	$\mathcal{O}_{\Sigma_{Xl}}(p_{67})^{3/4}$
Type IC	$(Xl + \overline{Xl})$	Σ_{Xl} (pinched)	$3H - E_6 - E_7$	1	$\mathcal{O}_{\Sigma_{Xl}}(p_{67})^{1/4}$	$\mathcal{O}_{\Sigma_{Xl}}(p_{67})^{-5/4}$
	$(Xh + \overline{Xh})$	Σ_{Xh} (pinched)	$3H - E_4 - E_7$	1	$\mathcal{O}_{\Sigma_{Xh}}(p'_{47})^{1/4}$	$\mathcal{O}_{\Sigma_{Xh}}(p'_{47})^{1/2}$
Type IIB	$(Xh + \overline{Xh})$	Σ_{Xh} (pinched)	$3H - E_6 - E_7$	1	$\mathcal{O}_{\Sigma_{Xh}}(p_{67})^{1/4}$	$\mathcal{O}_{\Sigma_{Xh}}(p_{67})^{1/2}$

TABLE XIV: The vector-like particle curves and the gauge bundle assignments for each curve in Type I and Type II models with two pairs of bulk vector-like particles (XT_i and \overline{XT}_i). Here, $p_{45} = p_4 - p_5$, $p_{67} = p_6 - p_7$, and $p'_{47} = p'_4 - p'_7$.

Models	Particles	Curve	Class	g_Σ	L_Σ	L_Σ^n
Type III	$(XF + \overline{XF})$	Σ_{XF} (pinched)	$3H - E_4 - E_5$	1	$\mathcal{O}_{\Sigma_{XF}}(p_{45})^{1/4}$	$\mathcal{O}_{\Sigma_{XF}}(p_{45})^{-1/4}$
	$(Xl_1 + \overline{Xl}_1)$	Σ_{Xl_1} (pinched)	$3H - E_1 - E_5$	1	$\mathcal{O}_{\Sigma_{Xf}}(p'_{15})^{1/4}$	$\mathcal{O}_{\Sigma_{Xf}}(p'_{15})^{-5/4}$
	$(Xl_2 + \overline{Xl}_2)$	Σ_{Xl_2} (pinched)	$3H - E_4 - E_7$	1	$\mathcal{O}_{\Sigma_{Xf}}(p'_{47})^{1/4}$	$\mathcal{O}_{\Sigma_{Xf}}(p'_{47})^{-5/4}$
	$(Xl_3 + \overline{Xl}_3)$	Σ_{Xl_3} (pinched)	$3H - E_2 - E_6$	1	$\mathcal{O}_{\Sigma_{Xf}}(p'_{62})^{1/4}$	$\mathcal{O}_{\Sigma_{Xf}}(p'_{62})^{-5/4}$
Type IIIA	$(Xl + \overline{Xl})$	Σ_{Xl} (pinched)	$3H - E_6 - E_7$	1	$\mathcal{O}_{\Sigma_{Xl}}(p_{67})^{1/4}$	$\mathcal{O}_{\Sigma_{Xf}}(p_{67})^{-5/4}$
Type IIIB	$(Xf + \overline{Xf})$	Σ_{Xf} (pinched)	$3H - E_6 - E_7$	1	$\mathcal{O}_{\Sigma_{Xf}}(p_{67})^{1/4}$	$\mathcal{O}_{\Sigma_{Xf}}(p_{67})^{3/4}$
Type IIID	$(Xh + \overline{Xh})$	Σ_{Xh} (pinched)	$3H - E_6 - E_7$	1	$\mathcal{O}_{\Sigma_{Xh}}(p_{67})^{1/4}$	$\mathcal{O}_{\Sigma_{Xh}}(p_{67})^{1/2}$

TABLE XV: The vector-like particle curves and the gauge bundle assignments for each curve in Type IIIA models with two pairs of bulk vector-like particles (XT_1 and \overline{XT}_1). Here, $p_{45} = p_4 - p_5$, $p_{67} = p_6 - p_7$, and $p'_{kl} = p'_k - p'_l$ for $kl = 15, 47, 62$.

Appendix D: Beta Functions for the Bulk Vector-Like Particles XT_i and \overline{XT}_i

In the convention of Ref. [62], we first present the one-loop beta functions $\Delta b \equiv (\Delta b_1, \Delta b_2, \Delta b_3)$ as complete supermultiplets from the vector-like particles XT_i and \overline{XT}_i in the supersymmetric Standard Model

$$\Delta b^{XT+\overline{XT}} = \left(\frac{39}{5}, 3, 3 \right). \quad (\text{D1})$$

Second, we present the two-loop beta functions from the vector-like particles XT_i and \overline{XT}_i

$$\Delta B^{XT+XT^c} = \begin{pmatrix} \frac{323}{25} & 15 & \frac{176}{5} \\ 5 & 21 & 16 \\ \frac{22}{5} & 6 & 34 \end{pmatrix}. \quad (\text{D2})$$

In the flipped $SU(5) \times U(1)_X$ models, we first present the one-loop beta functions $\Delta b \equiv (\Delta b_1, \Delta b_5)$ as complete supermultiplets from the vector-like particles XT_i and \overline{XT}_i

$$\Delta b^{XT+\overline{XT}} = (8, 3). \quad (\text{D3})$$

Second, we present the two-loop beta functions from the vector-like particles XT_i and \overline{XT}_i

$$\Delta B^{XT+\overline{XT}} = \begin{pmatrix} \frac{64}{5} & \frac{576}{5} \\ \frac{24}{5} & \frac{366}{5} \end{pmatrix}. \quad (\text{D4})$$

-
- [1] W. Buchmuller, K. Hamaguchi, O. Lebedev and M. Ratz, Phys. Rev. Lett. **96**, 121602 (2006), and references therein.
 - [2] O. Lebedev, H. P. Nilles, S. Raby, S. Ramos-Sanchez, M. Ratz, P. K. S. Vaudrevange and A. Wingerter, Phys. Lett. B **645**, 88 (2007), and references therein.
 - [3] J. E. Kim and B. Kyae, Nucl. Phys. B **770**, 47 (2007); Phys. Rev. D **77**, 106008 (2008); J. H. Huh, J. E. Kim and B. Kyae, arXiv:0904.1108 [hep-ph].
 - [4] V. Braun, Y. H. He, B. A. Ovrut and T. Pantev, Phys. Lett. B **618**, 252 (2005); JHEP **0605**, 043 (2006), and references therein.
 - [5] V. Bouchard and R. Donagi, Phys. Lett. B **633**, 783 (2006), and references therein.
 - [6] J. R. Ellis, S. Kelley and D. V. Nanopoulos, Phys. Lett. B **260**, 131 (1991); P. Langacker and M. X. Luo, Phys. Rev. D **44**, 817 (1991); U. Amaldi, W. de Boer and H. Furstenau, Phys. Lett. B **260**, 447 (1991).
 - [7] For a review, see K. R. Dienes, Phys. Rept. **287**, 447 (1997), and references therein.
 - [8] P. Horava and E. Witten, Nucl. Phys. B **460**, 506 (1996).

- [9] E. Witten, Nucl. Phys. B **471**, 135 (1996).
- [10] I. Antoniadis, J. R. Ellis, J. S. Hagelin and D. V. Nanopoulos, Phys. Lett. B **205** (1988) 459; Phys. Lett. B **208** (1988) 209 [Addendum-ibid. B **213** (1988) 562]; Phys. Lett. B **231** (1989) 65.
- [11] A. E. Faraggi, D. V. Nanopoulos and K. J. Yuan, Nucl. Phys. B **335**, 347 (1990).
- [12] I. Antoniadis, G. K. Leontaris and J. Rizos, Phys. Lett. B **245**, 161 (1990).
- [13] J. L. Lopez, D. V. Nanopoulos and K. J. Yuan, Nucl. Phys. B **399**, 654 (1993); D. V. Nanopoulos, hep-ph/0211128.
- [14] G. B. Cleaver, A. E. Faraggi, D. V. Nanopoulos and J. W. Walker, Nucl. Phys. B **620**, 259 (2002), and references therein.
- [15] M. Berkooz, M. R. Douglas and R. G. Leigh, Nucl. Phys. B **480**, 265 (1996).
- [16] L. E. Ibanez, F. Marchesano and R. Rabadan, JHEP **0111**, 002 (2001).
- [17] R. Blumenhagen, B. Kors, D. Lust and T. Ott, Nucl. Phys. B **616**, 3 (2001).
- [18] M. Cvetič, G. Shiu and A. M. Uranga, Phys. Rev. Lett. **87**, 201801 (2001); M. Cvetič, G. Shiu and A. M. Uranga, Nucl. Phys. B **615**, 3 (2001).
- [19] M. Cvetič, I. Papadimitriou and G. Shiu, Nucl. Phys. B **659**, 193 (2003) [Erratum-ibid. B **696**, 298 (2004)].
- [20] M. Cvetič, T. Li and T. Liu, Nucl. Phys. B **698**, 163 (2004). M. Cvetič, P. Langacker, T. Li and T. Liu, Nucl. Phys. B **709**, 241 (2005).
- [21] C.-M. Chen, G. V. Kraniotis, V. E. Mayes, D. V. Nanopoulos and J. W. Walker, Phys. Lett. B **611**, 156 (2005); Phys. Lett. B **625**, 96 (2005).
- [22] C. M. Chen, T. Li and D. V. Nanopoulos, Nucl. Phys. B **732**, 224 (2006).
- [23] R. Blumenhagen, M. Cvetič, P. Langacker and G. Shiu, Ann. Rev. Nucl. Part. Sci. **55**, 71 (2005), and references therein.
- [24] T. P. T. Dijkstra, L. R. Huiszoon and A. N. Schellekens, Phys. Lett. B **609**, 408 (2005).
- [25] T. P. T. Dijkstra, L. R. Huiszoon and A. N. Schellekens, Nucl. Phys. B **710**, 3 (2005), and references therein.
- [26] R. Blumenhagen, V. Braun, T. W. Grimm and T. Weigand, Nucl. Phys. B **815**, 1 (2009).
- [27] R. Blumenhagen, M. Cvetič and T. Weigand, Nucl. Phys. B **771**, 113 (2007); L. E. Ibanez and A. M. Uranga, JHEP **0703**, 052 (2007); R. Blumenhagen, M. Cvetič, D. Lust, R. Richter and T. Weigand, Phys. Rev. Lett. **100**, 061602 (2008).
- [28] C. M. Chen, T. Li, V. E. Mayes and D. V. Nanopoulos, Phys. Lett. B **665**, 267 (2008).
- [29] C. M. Chen, T. Li, V. E. Mayes and D. V. Nanopoulos, Phys. Rev. D **77**, 125023 (2008).
- [30] I. Gogoladze, T. Li, Y. Mimura and S. Nandi, Phys. Lett. B **622**, 320 (2005); Phys. Rev. D

- 72**, 055006 (2005).
- [31] C. Vafa, Nucl. Phys. B **469**, 403 (1996).
 - [32] R. Donagi and M. Wijnholt, arXiv:0802.2969 [hep-th].
 - [33] C. Beasley, J. J. Heckman and C. Vafa, JHEP **0901**, 058 (2009).
 - [34] C. Beasley, J. J. Heckman and C. Vafa, JHEP **0901**, 059 (2009).
 - [35] R. Donagi and M. Wijnholt, arXiv:0808.2223 [hep-th].
 - [36] J. J. Heckman, J. Marsano, N. Saulina, S. Schafer-Nameki and C. Vafa, arXiv:0808.1286 [hep-th].
 - [37] J. Marsano, N. Saulina and S. Schafer-Nameki, arXiv:0808.1571 [hep-th].
 - [38] J. Marsano, N. Saulina and S. Schafer-Nameki, arXiv:0808.2450 [hep-th].
 - [39] J. J. Heckman and C. Vafa, arXiv:0809.1098 [hep-th].
 - [40] A. Font and L. E. Ibanez, JHEP **0902**, 016 (2009).
 - [41] A. P. Braun, A. Hebecker, C. Ludeling and R. Valandro, Nucl. Phys. B **815**, 256 (2009).
 - [42] J. J. Heckman and C. Vafa, arXiv:0811.2417 [hep-th].
 - [43] J. Jiang, T. Li, D. V. Nanopoulos and D. Xie, arXiv:0811.2807 [hep-th].
 - [44] A. Collinucci, arXiv:0812.0175 [hep-th].
 - [45] R. Blumenhagen, Phys. Rev. Lett. **102**, 071601 (2009).
 - [46] J. J. Heckman, A. Tavanfar and C. Vafa, arXiv:0812.3155 [hep-th].
 - [47] J. L. Bourjaily, arXiv:0901.3785 [hep-th].
 - [48] H. Hayashi, T. Kawano, R. Tatar and T. Watari, arXiv:0901.4941 [hep-th].
 - [49] B. Andreas and G. Curio, arXiv:0902.4143 [hep-th].
 - [50] C. M. Chen and Y. C. Chung, arXiv:0903.3009 [hep-th].
 - [51] J. J. Heckman, G. L. Kane, J. Shao and C. Vafa, arXiv:0903.3609 [hep-ph].
 - [52] R. Donagi and M. Wijnholt, arXiv:0904.1218 [hep-th].
 - [53] V. Bouchard, J. J. Heckman, J. Seo and C. Vafa, arXiv:0904.1419 [hep-ph].
 - [54] L. Randall and D. Simmons-Duffin, arXiv:0904.1584 [hep-ph].
 - [55] J. J. Heckman and C. Vafa, arXiv:0904.3101 [hep-th].
 - [56] J. Marsano, N. Saulina and S. Schafer-Nameki, arXiv:0904.3932 [hep-th].
 - [57] J. L. Bourjaily, arXiv:0905.0142 [hep-th].
 - [58] S. M. Barr, Phys. Lett. B **112**, 219 (1982).
 - [59] J. P. Derendinger, J. E. Kim and D. V. Nanopoulos, Phys. Lett. B **139**, 170 (1984).
 - [60] I. Antoniadis, J. R. Ellis, J. S. Hagelin and D. V. Nanopoulos, Phys. Lett. B **194**, 231 (1987).
 - [61] J. L. Lopez and D. V. Nanopoulos, Phys. Rev. Lett. **76**, 1566 (1996).

- [62] J. Jiang, T. Li and D. V. Nanopoulos, Nucl. Phys. B **772**, 49 (2007).
- [63] K. Nakamura, Int. J. Mod. Phys. A **18**, 4053 (2003).
- [64] J. P. Conlon, JHEP **0904**, 059 (2009).
- [65] C. S. Huang, J. Jiang and T. Li, Nucl. Phys. B **702**, 109 (2004), and the references therein.
- [66] C. Amsler *et al.* [Particle Data Group], Phys. Lett. B **667**, 1 (2008).
- [67] Y. J. Huo, J. Jiang, T. Li, D. V. Nanopoulos, C. L. Tong, in preparation.
- [68] K. S. Babu, I. Gogoladze, M. U. Rehman and Q. Shafi, Phys. Rev. D **78**, 055017 (2008).
- [69] J. R. Ellis, D. V. Nanopoulos and J. Walker, Phys. Lett. B **550**, 99 (2002).
- [70] T. Li, D. V. Nanopoulos and J. Walker, in preparation.
- [71] J. R. Ellis, D. V. Nanopoulos and K. A. Olive, Phys. Lett. B **300**, 121 (1993); J. R. Ellis, J. L. Lopez, D. V. Nanopoulos and K. A. Olive, Phys. Lett. B **308**, 70 (1993).
- [72] M. Fukugita and T. Yanagida, Phys. Lett. B **174**, 45 (1986).
- [73] B. Kyae and Q. Shafi, Phys. Lett. B **635**, 247 (2006).
- [74] D. N. Spergel *et al.* [WMAP Collaboration], Astrophys. J. Suppl. **170**, 377 (2007).
- [75] S. Hu, T. Li and D. V. Nanopoulos, in preparation.